Static and Dynamic Behavior of Autocatalytic Replicators in Reactor Networks

ARTICLE *in* INDUSTRIAL & ENGINEERING CHEMISTRY RESEARCH · JUNE 2004

Impact Factor: 2.59 · DOI: 10.1021/ie030802d

4 AUTHORS, INCLUDING:

Eric Tatara
Argonne National Laboratory
42 PUBLICATIONS **441** CITATIONS
SEE PROFILE

Fouad Teymour
Illinois Institute of Technology
87 PUBLICATIONS **958** CITATIONS
SEE PROFILE

Ali Cinar
Illinois Institute of Technology
176 PUBLICATIONS **2,074** CITATIONS
SEE PROFILE

Static and Dynamic Behavior of Autocatalytic Replicators in Reactor Networks

Eric Tatara, Inanc Birol, Fouad Teymour, and Ali Çınar*

Department of Chemical and Environmental Engineering, Illinois Institute of Technology, 10 West 33rd Street, Chicago, Illinois 60616

The static and dynamic behavior of the autocatalytic reaction R + 2P → 3P with decay P → D is studied in networks of coupled continuous stirred tank reactors (CSTRs). Numerical bifurcation studies of the system are performed, resulting in rich steady-state bifurcation structures with multiple steady states and isolas. The heterogeneity of the networks is influenced by the number of reactors as well as the network topology. It is shown that the number of steady states of the network increases with heterogeneity, thereby allowing those autocatalytic species to exist in the network that would normally not exist in the homogeneous environment of a single CSTR. Spatial patterns of stable steady states are evident in reactor networks. Dynamic simulation studies are performed to illustrate the transition from one stable state configuration to another or from stable steady states to periodic regimes.

1. Introduction

When carried out in a continuous stirred tank reactor (CSTR), various classes of chemical reactions lead to complex and fascinating static and dynamic phenomena. These have been widely studied over the past few decades. Examples include autothermal reactions, autocatalytic reactions, and polymerizations. The analysis of Uppal and Ray[1] on the behavior of a CSTR with a nonisothermal reaction was one of the first thorough investigations of complex behavior in chemical reaction systems, extending some of the initial ideas presented by Bilous and Amundson.[2] Analytical solutions of the steady states and their stability characteristics show complex behavior, such as limit cycles. Further investigation of the nonisothermal system[3,4] using the reactor feed flow rate as a bifurcation parameter yields even more types of complex behavior, such as mushrooms and isolas.

The work of Lin[5] and Gray and Scott[6] on the isothermal autocatalytic reaction A + nB → (n + 1)B with decay B → C shows that cubic (n = 2) and quadratic (n = 1) autocatalytic reactions exhibit behavior similar to that of nonisothermal reactions. The solution multiplicities include isolas and mushrooms as well as limit cycles. Further work has determined how the various model parameters affect the stability criteria and conditions for multiplicity as well as a more sophisticated numerical analysis of the periodic solutions.[7] Reversibility of the cubic autocatalytic reaction scheme has been shown to have a significant effect on the shape of the bifurcation diagram and the regions of multistability.[8,9]

The first work to report the observation of chaos in a nonisothermal CSTR with cubic autocatalysis was that of Lynch.[10,11] The added parallel reaction E + 2B → D increases the model order to 3, which is a necessary condition for chaos in a continuous autonomous system. Essentially, there are now two kinds of substrates but still just one autocatalytic species. Up to five steady states can occur in this system. In the cited work, numerical solutions of the stable steady states are obtained as a function of the ratio of the substrate concentration in the feed to the species concentration in the feed (E_0/B_0). As the bifurcation parameter E_0/B_0 is changed, the system moves from a single steady state to period doubling to chaos. Within the chaotic regime are several "windows" of intermittent nonchaotic behavior. Further changes to the bifurcation parameter yield a change from chaos to period halving to a single steady-state solution.

Observations of solution multiplicity, sustained oscillations, and chaos have also been observed experimentally. Guderian et al.[12] report a phenomenon known as stochastic resonance in a CSTR with the well-known Belousov−Zhabotinsky reaction. While operating the system near a Hopf bifurcation point, noise is added to the input flow rate. Above some threshold, the CSTR spontaneously oscillates similarly to an excitable system. Essentially, the system is so close to the bifurcation point that a slight disturbance causes the system to temporarily shift into the oscillatory regime before settling down to the original steady state. Further observations of this phenomenon have been reported in the peroxidase−oxidase reaction scheme[13] as well as the minimal-bromate reaction[14] in a CSTR.

Birol and Teymour[15] have studied isothermal autocatalysis when two competing species are introduced to the system. It was shown that, with N species, although there may be as many as $2(2^N - 1)$ steady states, only one species can exist stably in the reactor as $t \to \infty$. Additionally, when the system hosts a robust autocatalytic species (continuously fed to the system and thus can never be washed out), the presence of an invading species can significantly decrease the host species concentration and a nonlinear control scheme is necessary to first remove the invading species and then return the host species to the original steady state.[16,17]

Polymerization systems also exhibit complex static and dynamic behavior. A recent paper[18] presents a review of these phenomena alongside an analysis of the effects at the root of the emergence of complex behavior.

* To whom correspondence should be addressed. Fax: (312) 567-8874. E-mail: cinar@iit.edu.

10.1021/ie030802d CCC: $27.50
Published on Web 06/04/2004

2. Reactor Networks

The effects of spatial heterogeneity on several reaction schemes carried out in a single CSTR may be studied by connecting several CSTRs together, such that material is exchanged between them. Lee et al.[19] studied the effect of micromixing on a CSTR with a cubic autocatalator. A stochastic process was employed to simulate the residence time of individual particles in the reactor. Large heterogeneities in the CSTR caused by imperfect mixing tended to destabilize limit cycles. This would suggest that further heterogeneity introduced to the system might cause similar changes in stability.

Several researchers have gone a step further and partitioned the system into several separate reactors. The Belousov−Zhabotinsky reaction scheme has been studied via physical experiments in networks of two or three reactors in both circular rings and linear arrays.[20−23] Lekebusch and Schneider[24] have studied mass-coupled biochemical oscillators using the peroxidase−oxidase reaction scheme. Yoshikawa and Fukunaga[25] have studied both the Briggs−Rauscher oscillator and the saltwater oscillator in a three-reactor network. Although much larger networks have not been studied experimentally, Hjelmfelt and Ross[26] have presented numerical results of simulating a 36-CSTR network with the bistable iodate−arsenous reaction scheme.

The method of mass exchange in most experiments is via diffusion or pumping in both physical experiments and computational simulation studies. Steady states as well as oscillatory states are found for a wide range of system parameters. Oscillatory states tend to synchronize as long as the frequency of the oscillations in each reactor are not too different, as is the case in many coupled oscillator systems.[27] Weak coupling of the reactors is usually employed because strong coupling of a reactor network causes the network to behave as one large reactor.

Laplante el al.[28] have studied the iodate−arsenous reaction in a network of eight CSTRs that are connected in a Hopfield-type network, where each reactor exchanges material with one another. The reactor network is able to "learn" or differentiate between different input patterns, in a manner similar to artificial neural networks (ANNs).[29] The connection strength between reactors function similarly to weights in an ANN. In addition to coupling via mass exchange, the reactors may be coupled via electrical potential.[30,31] It is theoretically possible to couple reactors via transmission of thermal energy such as with heat exchangers or with radiant energy such as light.[32] Strogatz[33] has compiled a detailed study of general works on coupled oscillators and complex oscillator networks in the physics and biology literature.

Taylor and Kevrekidis[34] have used numerical bifurcation techniques on the nonisothermal A → B system to understand the relationship between strong and weak coupling strengths. Each reactor, if isolated, can normally display periodic behavior for the parameter space of interest. Strong coupling between reactors causes the system to act as a single large reactor. Weak coupling allows the reactors to resonate at certain values of the bifurcation parameter (flow rate to one reactor) when the ratios of the oscillations in the uncoupled case are close to an integer ratio, e.g., 1:2 coupling. Large ratios of the oscillation frequency display behavior that is nearly indiscernible from quasi-periodic behavior. Additionally, if the oscillations are sufficiently "detuned", the phenomenon of phase death may occur, which means that two reactors that would normally operate on a periodic solution when uncoupled converge to a steady state when coupled.

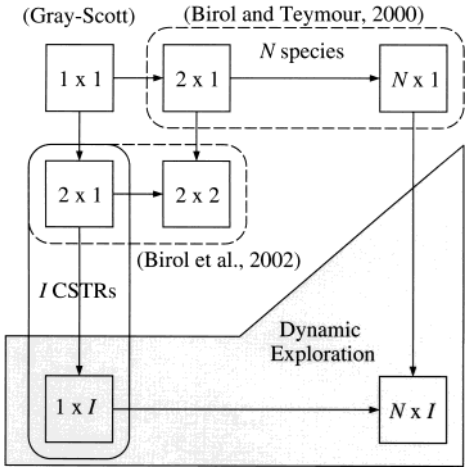

Figure 1. Graphical representation of network configurations.

The work of Birol et al.[35] investigates two and three reactor configurations, this time with competing cubic autocatalytic reactions. It was found that competitive coexistence occurs when the reactor is partitioned. Additionally, it was found that certain species that could not survive in a single CSTR were able to survive in the new heterogeneous environment, suggesting that spatial heterogeneity enlarges the boundaries of species survival. Furthermore, it was shown that the number of steady states increases exponentially with the size of the system.

This work examines the effects of introducing further spatial heterogeneity in networks hosting a single autocatalytic species. By constructing a graphical summary consisting of the number of CSTRs in the network versus the number of autocatalytic species in the network, one can observe how the previous work relates to current and future work (Figure 1). The original work by Gray and Scott[6] investigated a single autocatalytic species in a single CSTR as indicated in the upper left corner of Figure 1. Birol and Teymour[15] investigated *n* species in a single reactor, which encompasses the entire first row of Figure 1. Birol et al.[35] have increased the size of the network to incorporate two and three reactors hosting two competing species.

As the number of reactors and species increases, the solution of the state equations becomes analytically intractable because the number of roots of the resulting polynomial solution grows exponentially with the size of the system. Therefore, analysis of systems larger than those composed of two or three CSTRs better exploits computational methods to solve the equations. Even traditional numerical bifurcation techniques fail because of the extreme solution multiplicity of the system, necessitating a statistical approach to map the steady states of the system. Dynamic behavior may only be examined by exploration of the system via numerical simulation studies.

The next logical step in mapping the behavior of these systems is to examine a single autocatalytic species in networks of more than two reactors. The system presented in the next section involves a single autocatalytic species occupying networks of multiple reactors. Steady-state bifurcation structures are obtained for these

systems, and the dynamic behavior is examined through numerical simulation studies.

3. Reactor Network Model

A network of I interconnected CSTRs can be modeled by specifying the mass balance for an individual reactor at position i in the network, where $i = 1, .., I$. Figure 2 shows two possible interconnections for a system of four CSTRs. The cubic autocatalytic reaction for a single autocatalytic species is

$$\mathrm{R} + 2\mathrm{P} \xrightarrow{k} 3\mathrm{P} \quad (1)$$

$$\mathrm{P} \xrightarrow{k_\mathrm{d}} \mathrm{D} \quad (2)$$

R is the resource, P is the species, D is a dead (inert) species, k is the species growth rate constant, and k_d is the species death rate constant.

The production rates of the resource and species can then be written for a generic bidirectional ring network of size I

$$V\frac{\mathrm{d}R_i}{\mathrm{d}t'} = -VkR_iP_i^2 + F(R_0 - R_i) + G(R_{i-1} + R_{i+1} - 2R_i) \quad (3)$$

$$V\frac{\mathrm{d}P_i}{\mathrm{d}t'} = VkR_iP_i^2 - P_i(F + Vk_\mathrm{d}) + G(P_{i-1} + P_{i+1} - 2P_i) \quad (4)$$

where R_0 is the resource concentration in the feed, R_i is the resource concentration in reactor i, P_i is the species concentration in reactor i, F is the feed flow rate, G is the interconnection flow rate, and V is the reactor volume. The feed stream contains only the resource. The state equations can be written in dimensionless form as

$$\frac{\mathrm{d}r_i}{\mathrm{d}t} = -kr_ip_i^2 + f(1 - r_i) + g(r_{i-1} + r_{i+1} - 2r_i) \quad (5)$$

$$\frac{\mathrm{d}p_i}{\mathrm{d}t} = kr_ip_i^2 - p_i(f + d) + g(p_{i-1} + p_{i+1} - 2p_i) \quad (6)$$

by redefining the variables as $r_i = R_i/R_0$, $p_i = P_i/R_0$, $f = F/VR_0^2$, $g = G/VR_0^2$, $d = k_\mathrm{d}/R_0^2$, and $t = R_0^2t'$. For $i > 3$, analytical solutions become intractable, although it should be noted that a single trivial steady state ($r_i = 1$, $p_i = 0$) exists as $\forall\ i$ for every combination of model parameter values. This state represents total extinction in the system.

The geometry of the reactor network may depend on the number of reactors as well as the values of the interconnection flow rates. Figure 2a shows a bidirectional ring-shaped network in which all interconnection flow rates are equal. Ring-shaped networks do not have a starting or ending point, and thus any behavior attributed to a specific reactor ordering can be duplicated by arbitrarily rotating the reactor numbering. When all of the interconnection flow rates are equal, symmetry is present in the system. However, if the interconnection flow rates are limited to a single direction (Figure 2b), the symmetry is broken. Without loss of generality, the direction of interconnection flow in unidirectional networks will always be considered to be counterclockwise, or from reactor $i + 1$ to reactor i.

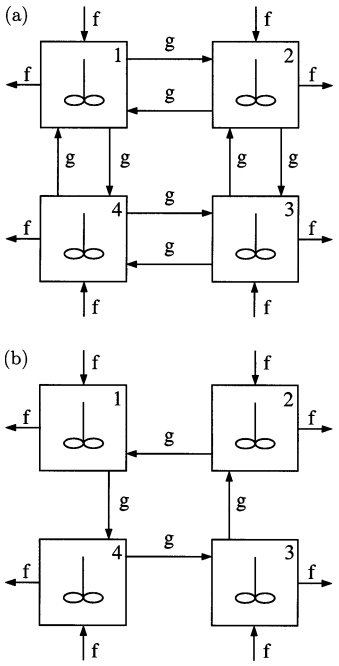

Figure 2. Types of CSTR networks: (a) a four-CSTR bidirectional ring network; (b) a unidirectional ring network.

The feed flow rates and interconnection flow rates are treated as manipulated variables. In the case studies presented later, either one is varied. Because the flow rates are only varied globally, no special considerations are necessary for conservation of mass. Each reactor has a feed inlet and outlet that are always equal, and each reactor has as many inlet as outlet interconnection streams that are always equal. Other variants of this problem with unequal flow rates will not be considered here.

4. Numerical Bifurcation Analysis

In some of the previous work on autocatalytic replicators in a CSTR, the bifurcation structure and its stability characteristics have been obtained via analytical solution of the state equations. In the case of multiple CSTRs and species, the analytical solution would result in a polynomial of order greater than 10^2 and occasionally greater that 10^3. Because larger systems are analytically intractable, a numerical method is required to obtain the steady-state bifurcation structure.

Numerical continuation software such as AUTO[36] and CONTENT[37] currently consists of a graphical or textual interface to a set of continuation libraries. The user supplies a set of steady states obtained from a nonlinear solver as the starting point for the continuation as well as a number of parameters specific to the numerical techniques used by the software. These parameters include information such as the solver tolerance or continuation step size limits and are highly problem-dependent and so must be chosen carefully or the continuer will fail to converge.

After significant experimentation to find a suitable set of parameters, a single solution branch for a single steady state can be computed. It should be noted that, to obtain the complete bifurcation diagram for the desired system parameter space, the continuation software parameters must often be altered to achieve convergence. The procedure for tracking steady states

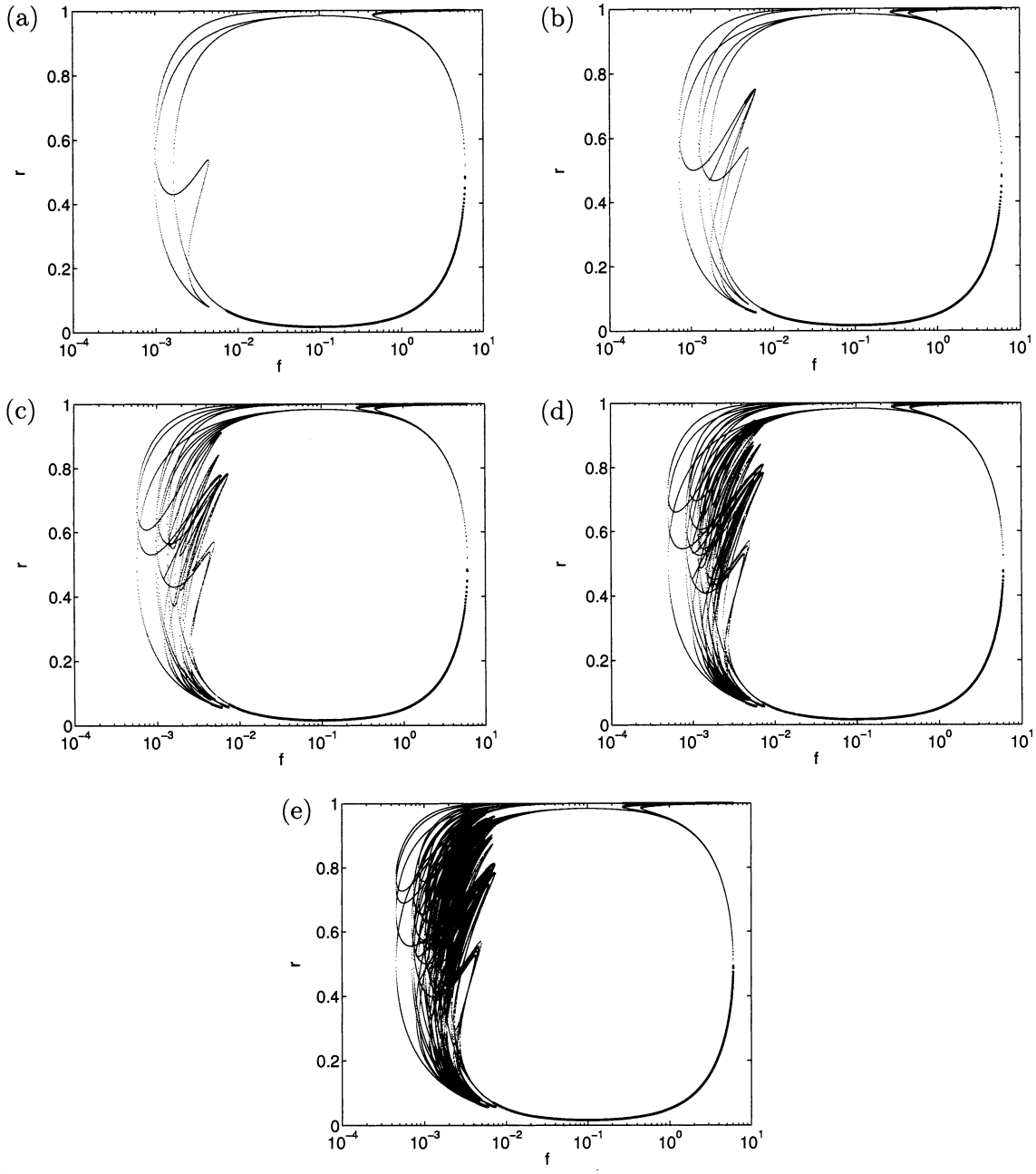

Figure 3. Bifurcation diagram of r vs f for bidirectional ring networks with $k = 25$, $d = 0.1$, and $g = 0.002$. The number of CSTRs in the network is (a) 2, (b) 3, (c) 4, (d) 5, and (e) 6. Unstable steady states are indicated with light lines, and stable steady states are indicated with dark lines.

is independent of that for tracking periodic solutions, which requires a separate set of numerical routines and parameters altogether.

Unfortunately, highly complex systems exhibit multiplicity of steady states and isolated solution branches that makes bifurcation analysis using such tools difficult. The user must perform the same difficult and time-consuming procedure for each solution curve, changing the continuation parameters as necessary to achieve convergence. Therefore, the problem becomes one of solution management. Current bifurcation software and computer hardware are sufficient for tracking a small number of solution branches, even for systems of 10^6 ordinary differential equations. Solution multiplicity is the complicating factor in bifurcation analysis, not the number of state equations.

Furthermore, the system of autocatalytic replicators in a CSTR network displays an unusually large number of multiple steady states. These types of systems are atypical of those usually studied via bifurcation analysis and therefore provide unique challenges. In a manner similar to that of Ourique et al.,[38] the nonlinear solver KINSOL[39] is used to map out a system without any a priori knowledge of the bifurcation structure. All of the steady-state solutions are found by sweeping the bifurcation parameter through the region of interest and using a large number of randomized initial guesses for the states. While this method is more computationally demanding than traditional numerical continuation methods, the fact that it works autonomously yields faster results than those methods that require repeated user input. Obtaining a complex bifurcation diagram using traditional continuation techniques would require an expert user several days to complete, whereas using a statistical technique requires only minutes on a 2 GHz

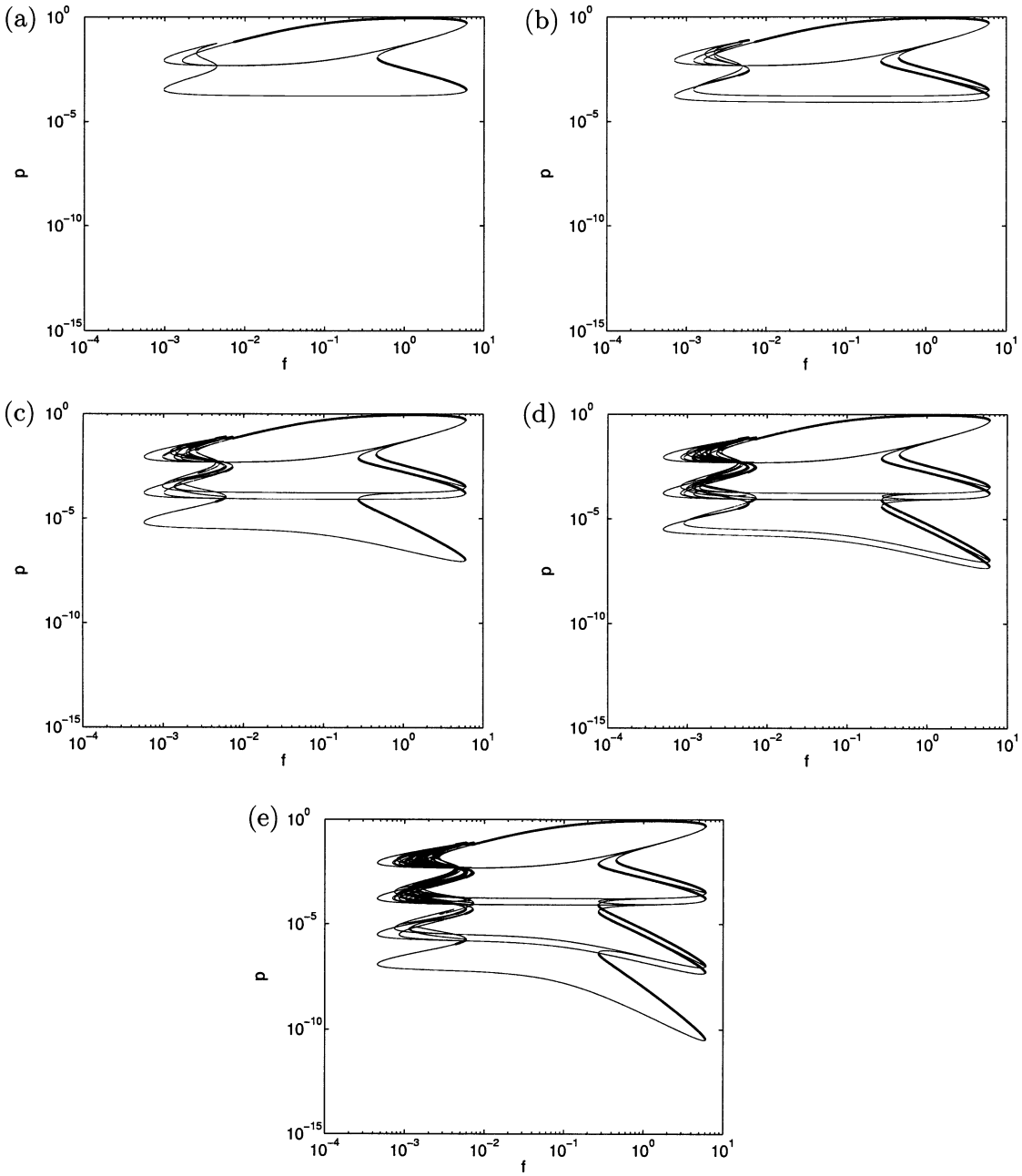

Figure 4. Bifurcation diagram of p vs f for bidirectional ring networks with $k = 25$, $d = 0.1$, and $g = 0.002$. The number of CSTRs in the network is (a) 2, (b) 3, (c) 4, (d) 5, and (e) 6. Unstable steady states are indicated with light lines, and stable steady states are indicated with dark lines.

PC. Additionally, statistical methods are far less likely to miss isolated solution branches.

After the steady-state bifurcation diagram is obtained by solving the set of nonlinear algebraic equations, the stability information is obtained by examining the eigenvalues of the Jacobian matrix. The analytical form of the Jacobian can be obtained for any combination of species in any network topology (see work by Birol et al.[35] for a sample case).

5. Steady-State Bifurcation Structure

The steady-state bifurcation diagram of r versus f for a single species in several different sized bidirectional ring networks is shown in Figure 3. The bifurcation diagrams are constructed for all possible steady-state values of r and p, thus the omission of the reactor number subscript, i. The resource and species concentration steady states in the bifurcation diagrams represent those values that *can* occur in an individual reactor but not the spatial arrangement of the steady states in the network. Larger networks permit a larger domain of existence not only with respect to the bifurcation parameter, in this case the feed flow rate, but also with respect to the resource concentration. A species can therefore exist in many more possible stable steady states and feed flow rates within larger networks than within smaller networksbecause of the increased spatial heterogeneity of the system. Although much of the bifurcation diagram is dominated by a large number of unstable steady states, there exist a number of stable steady states for a large range of feed flow rates. In addition to the single-CSTR steady states that are omnipresent in larger networks, the network exhibits

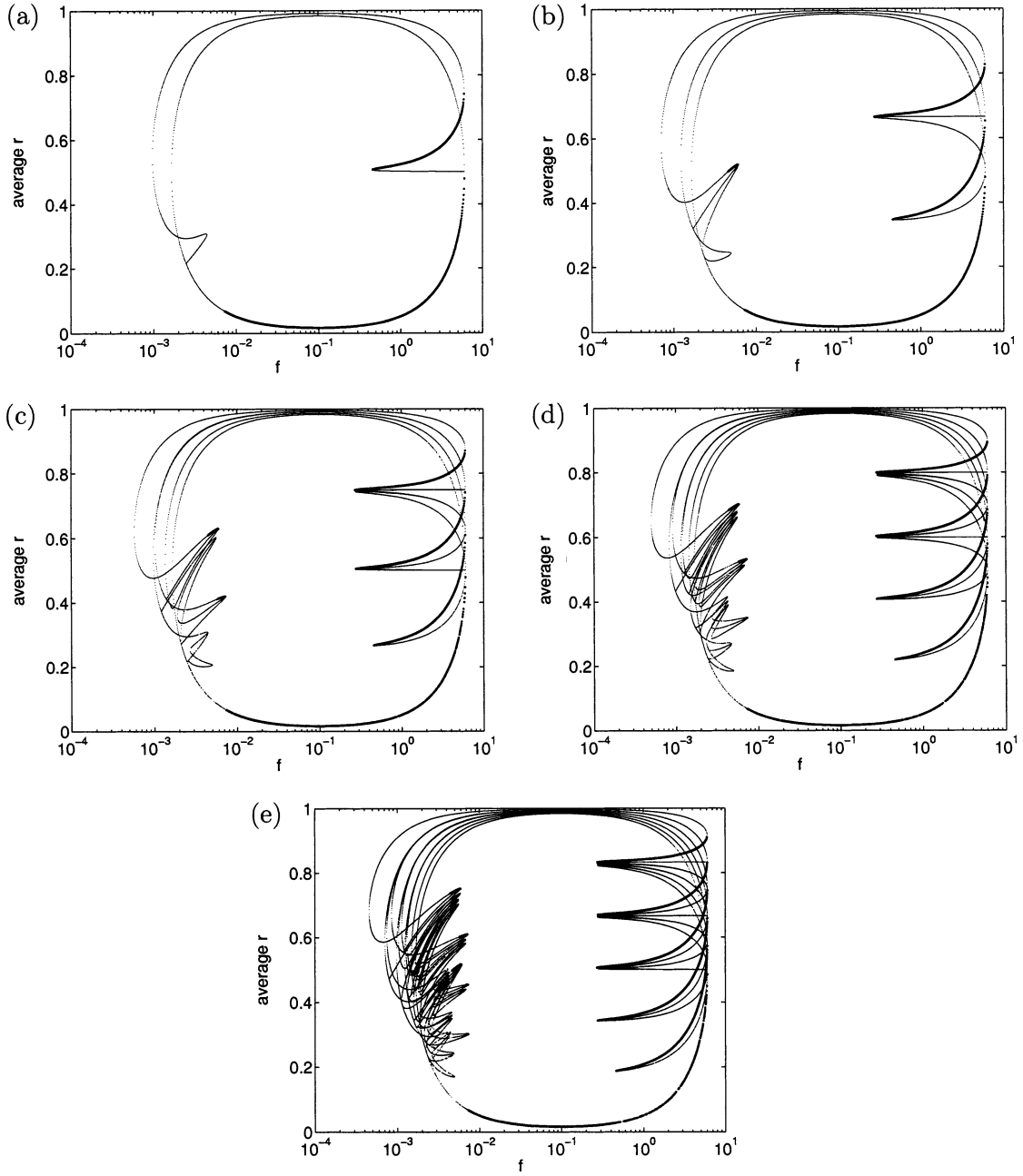

Figure 5. Bifurcation diagram of network average r vs f for bidirectional ring networks with $k = 25$, $d = 0.1$, and $g = 0.002$. The number of CSTRs in the network is (a) 2, (b) 3, (c) 4, (d) 5, and (e) 6. Unstable steady states are indicated with light lines, and stable steady states are indicated with dark lines.

multistability at low and high flow rates that are unique to networks of more than one reactor.

The corresponding bifurcation diagrams of p versus f are shown in Figure 4 on a log−log scale. Note that the high species concentrations in Figure 4 are related to the low resource concentrations in the respective configuration of Figure 3 because of a high rate of resource consumption of a populous species. Interestingly, the species concentration for some configurations remains nearly constant throughout the range of the bifurcation parameter, as is evident in the long nearly horizontal branches in species concentration. The autocatalytic species has stable steady states at concentration values as low as 10^{-10} for the six-CSTR network in contrast to the two-CSTR network, which only seems to support stable steady states at values greater than 10^{-3}. Also, this minimum attainable steady-state species concentration steps down logarithmically with increasing network size. However, the jump is more profound when going from an odd network size to an even one.

Initial examination of the steady-state bifurcation diagrams might suggest that, for large networks, there may be a large number of spatial combinations of stable steady-state resource and species concentrations. However, the bifurcation diagrams for the network average resource (Figure 5) and species concentrations (Figure 6) reveal that there actually are a smaller number of spatial combinations of stable steady states. For example, Figure 5b reveals that for the three-CSTR network there is only a single combination of stable steady states $(r_1, r_2, r_3) \approx (0.7, 0.06, 0.7)$ at low feed flow rates and two combinations (0.99, 0.99, 0.04) and (0.99, 0.04, 0.04) at high feed flow rates, in addition to those of the single CSTR. Moving to the four-CSTR network (Figure 5c), one can observe two pairs of stable steady states $(r_1, r_2, r_3, r_4) \approx (0.75, 0.9, 0.75, 0.06)$ and (0.77,

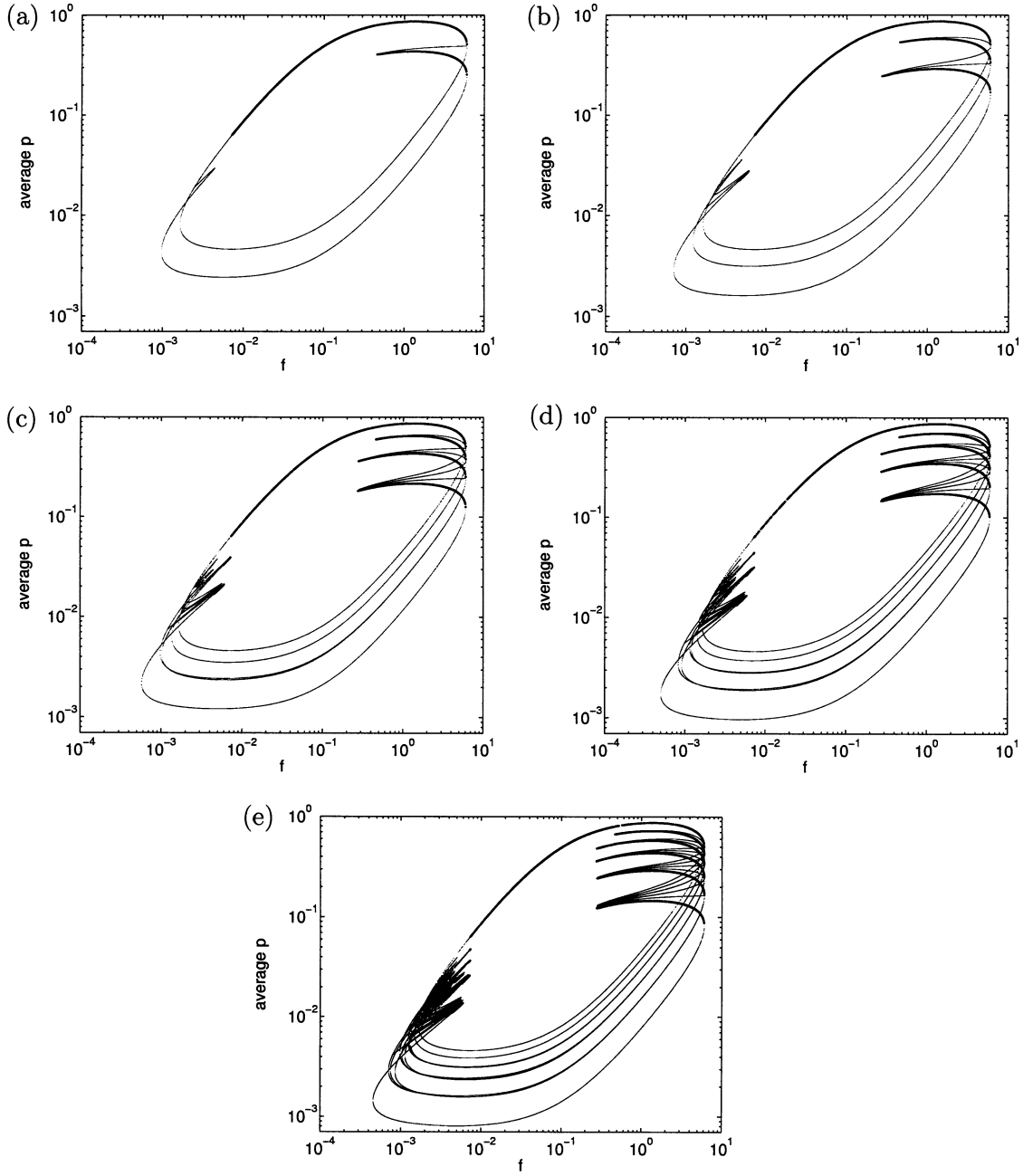

Figure 6. Bifurcation diagram of network average p vs f for bidirectional ring networks with $k = 25$, $d = 0.1$, and $g = 0.002$. The number of CSTRs in the network is (a) 2, (b) 3, (c) 4, (d) 5, and (e) 6. Unstable steady states are indicated with light lines, and stable steady states are indicated with dark lines.

0.06, 0.06, 0.77) at low feed flow rates and three combinations (0.99, 0.99, 0.99, 0.04), (0.99, 0.99, 0.04, 0.04), and (0.99, 0.04, 0.04, 0.04) at high feed flow rates.

Of note is an emergent phenomenon that is observed in the four-CSTR network is that of two reactors functioning as a single reactor. The stable steady states in the four-CSTR at low feed flow rates occur in two combinations. The first is a gradient-like pattern consisting of a high resource reactor surrounded by two intermediate resource reactors and finally a low resource reactor. The second pattern consists of two reactors with a high resource concentration and two with a low resource concentration. However, the reactor pairs are always adjacent to one another in the network. Thus, combinations of reactors 1 and 2 with a high resource and 3 and 4 with a low resource are possible but not an alternating combination of high and low resource combinations. Because this phenomenon occurs as a result of reactor coupling, the two coupled reactors functioning as a single large reactor must be in direct communication with one another via the interconnection flow rates. This phenomenon can occur when the number of reactors in the network is nonprime. The four-CSTR network can function as a two-CSTR network when two pairs of two reactors couple. Similarly, the six-CSTR network can function both as a two-CSTR network when two sets of three reactors couple and as a three-CSTR when three sets of two reactors couple. In contrast, the three-, five-, and seven-CSTR networks are all prime and do not contain any subsets.

A second emergent behavior of multireactor networks is apparent in the average resource bifurcation diagram (Figure 5). At high flow rates, the average network resource concentration has stable branches with concentrations that approach rational values. For example, the network average resource concentration for a two-

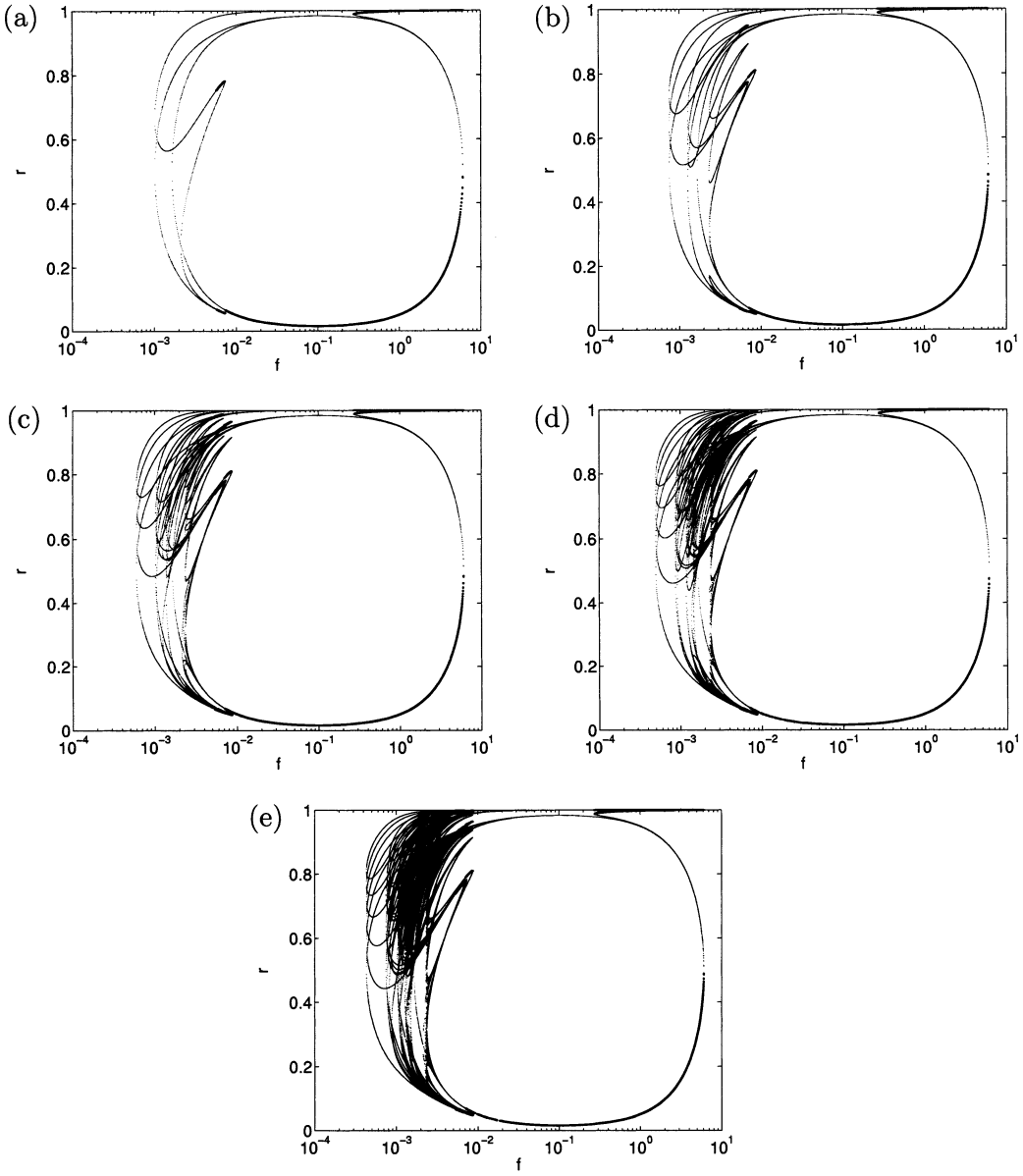

Figure 7. Bifurcation diagram of r vs f for unidirectional ring networks with $k = 25$, $d = 0.1$, and $g = 0.002$. The number of CSTRs in the network is (a) 2, (b) 3, (c) 4, (d) 5, and (e) 6. Unstable steady states are indicated with light lines, and stable steady states are indicated with dark lines.

CSTR network (Figure 5a) has a stable resource concentration of around $^1/_2$. The three-CSTR network (Figure 5b) has stable resource concentrations of around $^2/_3$ and $^1/_3$. The four-CSTR network (Figure 5c) has stable resource concentrations of around $^3/_4$, $^2/_4$, and $^1/_4$. This behavior is also evident in larger networks and occurs because, at high flow rates, the resource concentration is very close to either 0 or 1. For instance, in a two-CSTR network, if one reactor has a very high resource and the other has a very low resource concentration, then the network average will be about $^1/_2$. For a three-CSTR network, we have the possibility of either two reactors with high resource concentration or one reactor with high resource concentration, resulting in averages of approximately $^2/_3$ and $^1/_3$, respectively. We can easily generalize this for a network of I reactors, where the network average resource concentration may be near i/I, with $i = 1, ..., I$.

Next, the steady-state bifurcation structure of a network with unidirectional interconnection flow rates is investigated. Figure 7 shows how it differs from that of the case of bidirectional interconnection flow rates. The region of existence with respect to the feed flow rate of the single species is seen to decrease from the bidirectional case. However, it is evident from the larger number of stable steady states that the region of existence with respect to the resource and species concentrations has increased significantly. Additionally, the two-CSTR case (Figure 7a) now displays a pair of stable steady states at low feed flow rates, whereas in the bidirectional case, no stable steady states exist on the corresponding branch.

The two-CSTR case is unique among the other network topologies because the bidirectional and unidirectional configurations can be equivalent depending on the value of the interconnection flow rate. The two-CSTR bidirectional case consists of two reactors with interconnection flows between them and an additional set of interconnection flows imposed by the toroidal network boundary conditions. The two-CSTR unidirectional case, however, has only the unidirectional flow from one reactor to another and the single unidirectional

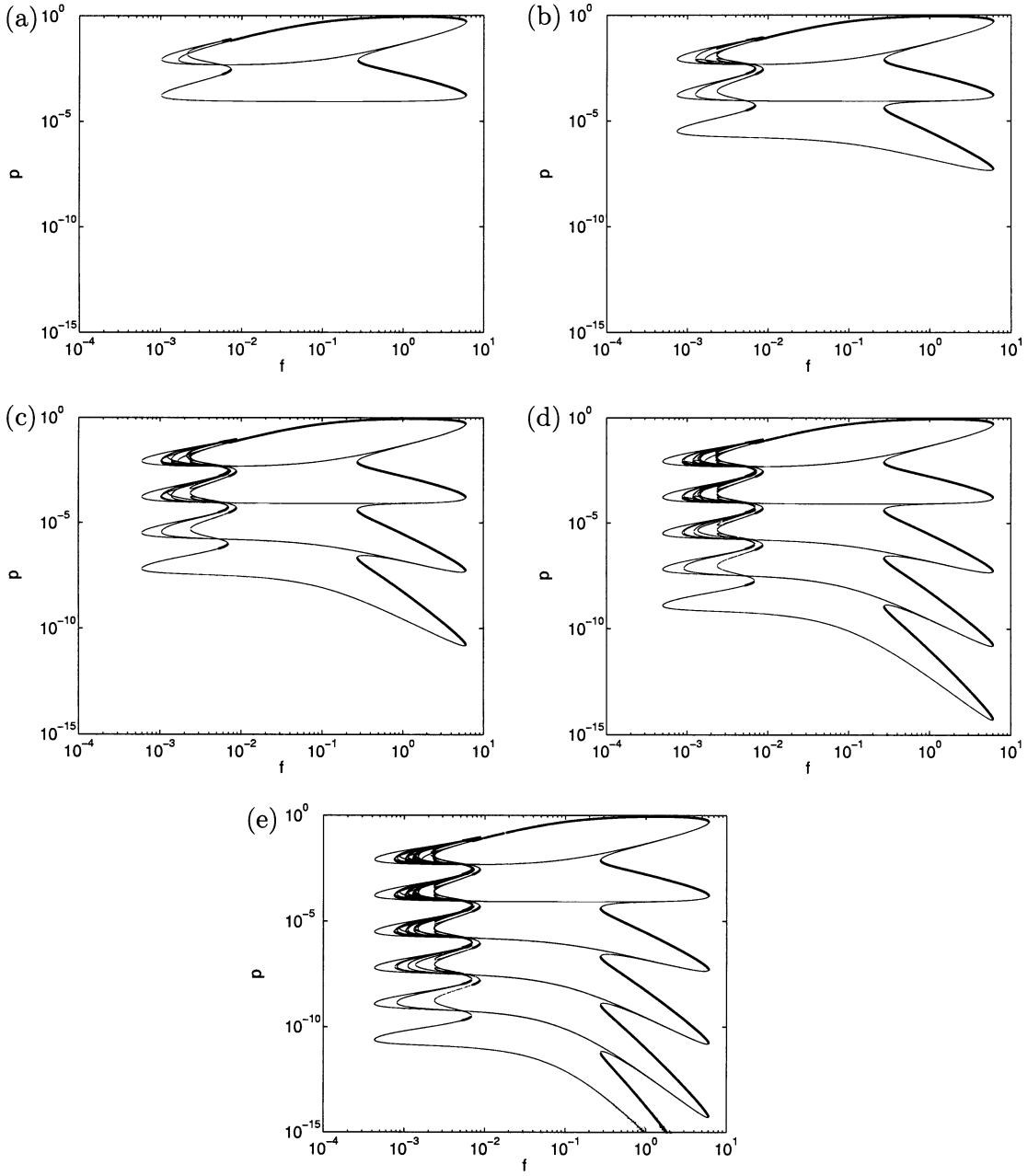

Figure 8. Bifurcation diagram of p vs f for unidirectional ring networks with $k = 25$, $d = 0.1$, and $g = 0.002$. The number of CSTRs in the network is (a) 2, (b) 3, (c) 4, (d) 5, and (e) 6. Unstable steady states are indicated with light lines, and stable steady states are indicated with dark lines.

flow imposed by the boundary conditions. Therefore, for a two-CSTR bidirectional network with interconnection flow rate g_2, there exists an equivalent two-CSTR unidirectional network with interconnection flow rate g_1, when $g_2 = 2g_1$.

As with bidirectional networks, unidirectional networks can support extremely low species concentrations. For the six-CSTR unidirectional network (Figure 8e), the lowest species concentration is below 10^{-15}, which is beyond the tolerance of the numerical solver. Similar to the bidirectional case, in unidirectional networks the minimum attainable steady-state species concentration jumps down logarithmically. Yet, unlike the bidirectional case, this jump is more or less uniform for even and odd network sizes. The bifurcation diagrams of the network average resource (Figure 9) and species (Figure 10) concentrations illustrate that not only are there more stable steady states than in the bidirectional case but there are more combinations of stable steady states at low feed flow rates.

In addition to limiting the interconnection flow rate to a single direction, the interconnection flow rate can be varied to introduce more or less spatial heterogeneity to the network. The effects of the interconnection flow rate on the steady-state behavior of bidirectional networks can be observed in Figure 11. The horizontal lines in the bifurcation diagram represent the steady states of the single-CSTR case and the trivial solution ($r = 1$). The steady states of the system approach the single-CSTR steady states at very low interconnection flow rates because each of the reactors behaves almost independently of the others. The same behavior is observed at high interconnection flow rates as the network effectively becomes one large CSTR. Between the two extreme values of the interconnection flow rates, a large number of steady states can be observed. As the

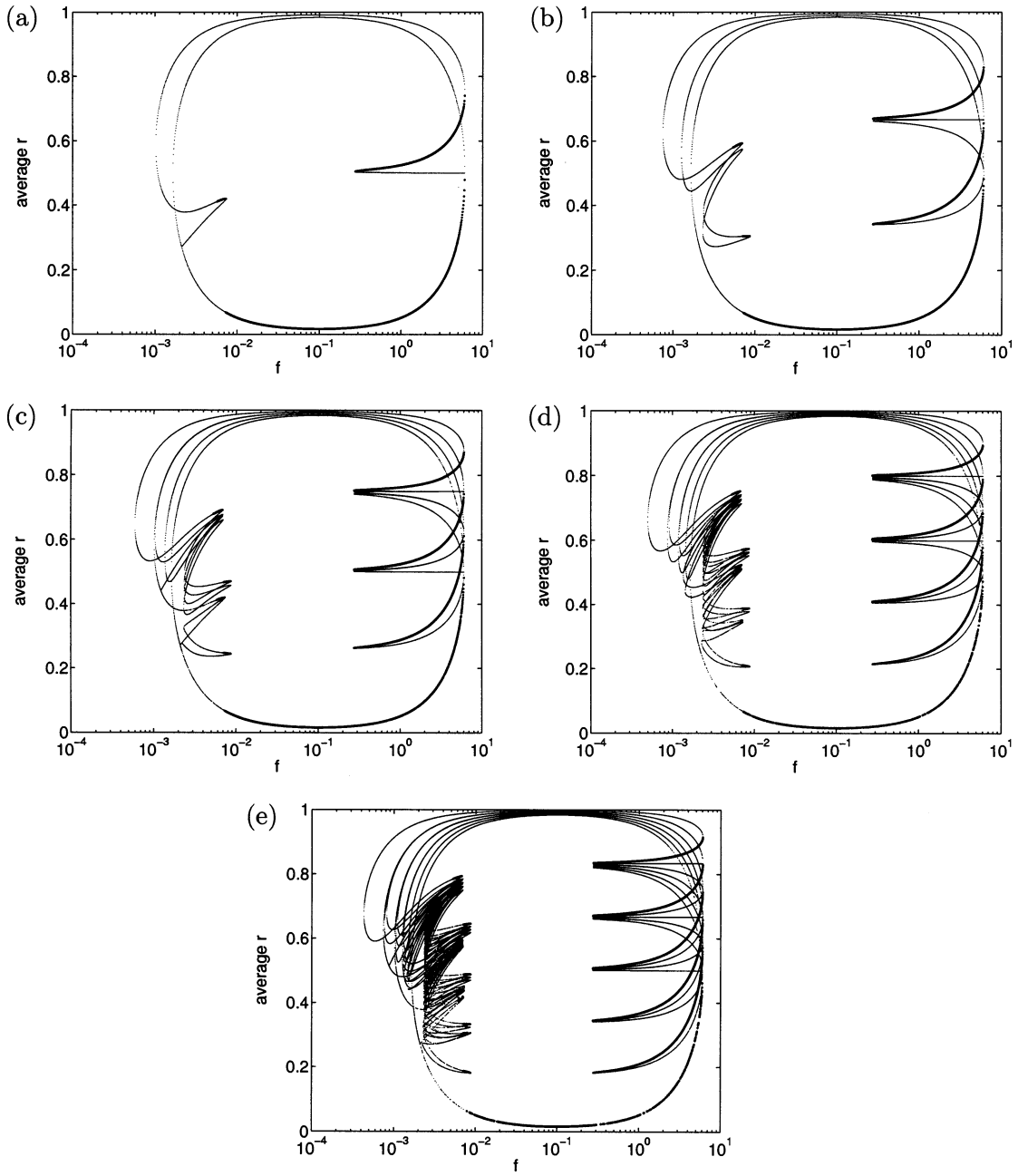

Figure 9. Bifurcation diagram of network average r vs f for unidirectional ring networks with $k = 25$, $d = 0.1$, and $g = 0.002$. The number of CSTRs in the network is (a) 2, (b) 3, (c) 4, (d) 5, and (e) 6. Unstable steady states are indicated with a light line and stable steady states are indicated with a dark line.

network becomes larger, the distribution of steady states appears to approach a continuum. For the example case shown in Figure 11, no stable steady states can be observed. As mentioned previously in the analysis of the steady-state bifurcation structure, networks that are multiples of smaller networks contain all of the steady states of the smaller networks. For example, a network of six CSTRs contains all of the steady states of the three-CSTR network and all of the steady states of the two-CSTR network in addition to those steady states that are unique to the six-CSTR network. Again, the single-CSTR steady states are omnipresent in any network.

Unidirectional networks display similar behavior when the interconnection flow rate is varied. Figure 12 shows the bifurcation diagram of r vs g/f for unidirectional networks. As with bidirectional networks, the steady states show a convergence to the single-CSTR case when the interconnection flow rate is very high or low. The emergence of stability between $g/f \approx 4.50$ and $g/f \approx 13.61$ in the six-CSTR case (Figure 12e) is also an important distinguishing characteristic of the unidirectional network. Note that for the bidirectional network with the same operating conditions, no stable steady states are present in the system. The six-CSTR network contains exactly six stable steady states, excluding the trivial steady state at $r = 1$. Each of the steady states corresponds to a single reactor, and the system exhibits a single spatial pattern. If one of the CSTRs is arbitrarily selected to be the *first* reactor that contains the highest resource concentration, then the reactors in the direction of flow away from the first reactor will have progressively higher resource concentrations. This also means that the species concentration decreases in the direction of flow. In this fashion, the upstream reactors can act as a species inflow source to the downstream

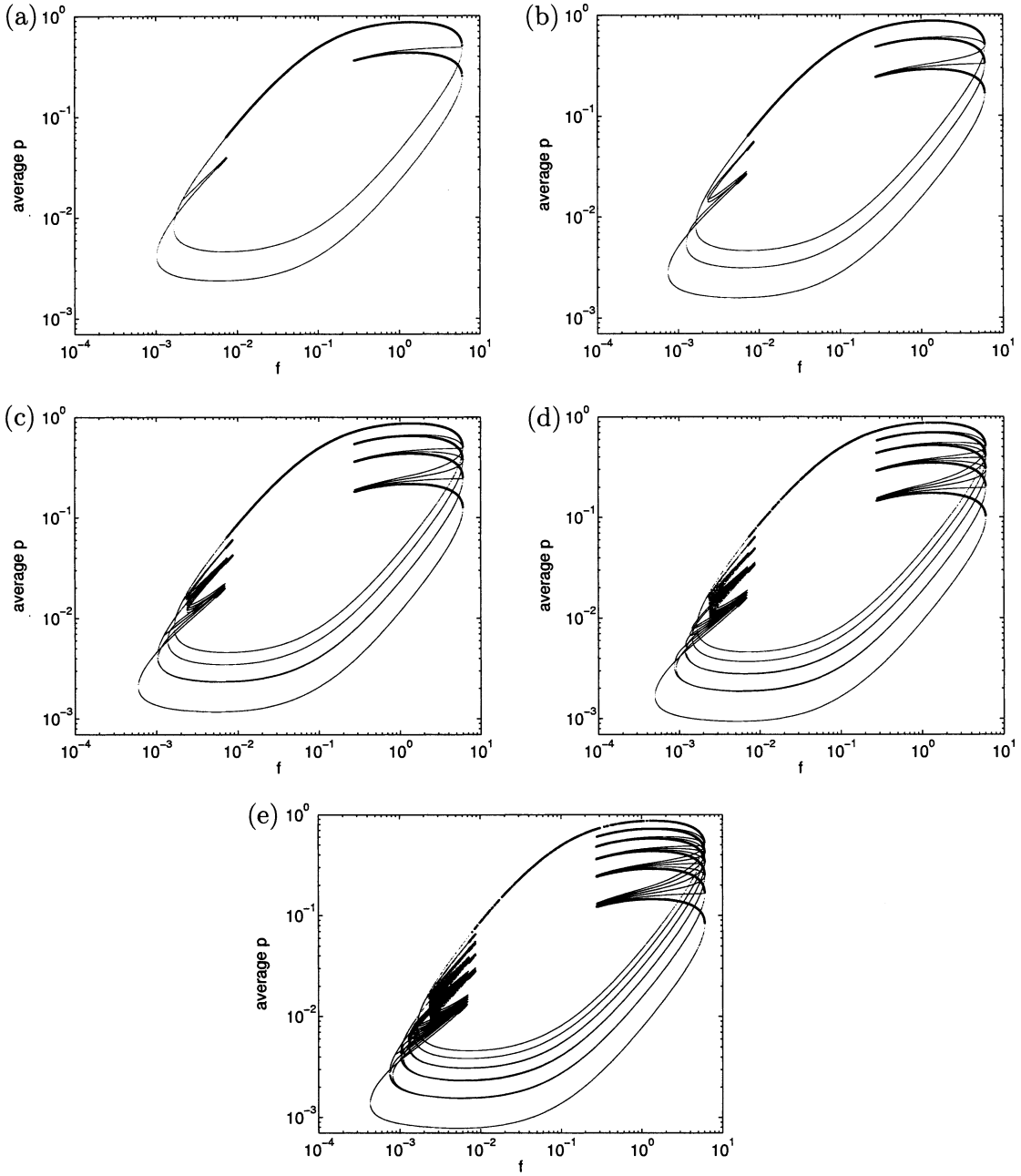

Figure 10. Bifurcation diagram of network average p vs f for unidirectional ring networks with $k = 25$, $d = 0.1$, and $g = 0.002$. The number of CSTRs in the network is (a) 2, (b) 3, (c) 4, (d) 5, and (e) 6. Unstable steady states are indicated with light lines, and stable steady states are indicated with dark lines.

reactors. The species concentration in the *last* reactor is very small. Hence, even though it is fed to the first reactor, its contribution is very small. As the size of the network is increased to seven CSTRs (Figure 12f), the region of stability increases beyond that of the six-reactor system from $g/f \approx 3.53$ to $g/f \approx 19.82$. Furthermore, something interesting occurs: the lowest two stable branches of the resource bifurcation diagram cross at $g/f \approx 16.71$; thus, the trend of decreasing species concentration in the direction of flow is broken.

In addition to more stable steady states, larger networks permit autocatalytic species to exist in cases where smaller networks do not. As the feed flow rate is reduced from $f = 0.002$ in the example shown in Figure 12, the two horizontal steady states converge and disappear from the bifurcation diagram completely. Thus, the system experiences a transition from single-species existence to extinction in a single-CSTR setup. Figure 13 shows the bifurcation diagram for the unidirectional ring network just as the single-CSTR steady states disappear for $f = 0.001\,65$. Clearly, steady states exist in CSTR networks of multiple reactors, whereas the single CSTR has none. When the size of the network is increased to seven reactors (Figure 13f), a stable region occurs between $g/f \approx 6.43$ and $g/f \approx 15.54$, in contrast to the single-CSTR case that has no steady states for the same set of parameters.

Reducing the feed flow rate further to $f = 0.001\,25$ yields the bifurcation structure shown in Figure 14. The long, drawn out steady-state structures of the previous examples now appear as oval-shaped isolas. At this feed flow rate, the range of steady states with respect to the interconnection flow rate is smaller than that with higher feed flow rates. Furthermore, the emergence of stability requires a network containing nine CSTRs (Figure 14h). The 9-CSTR network has stable steady

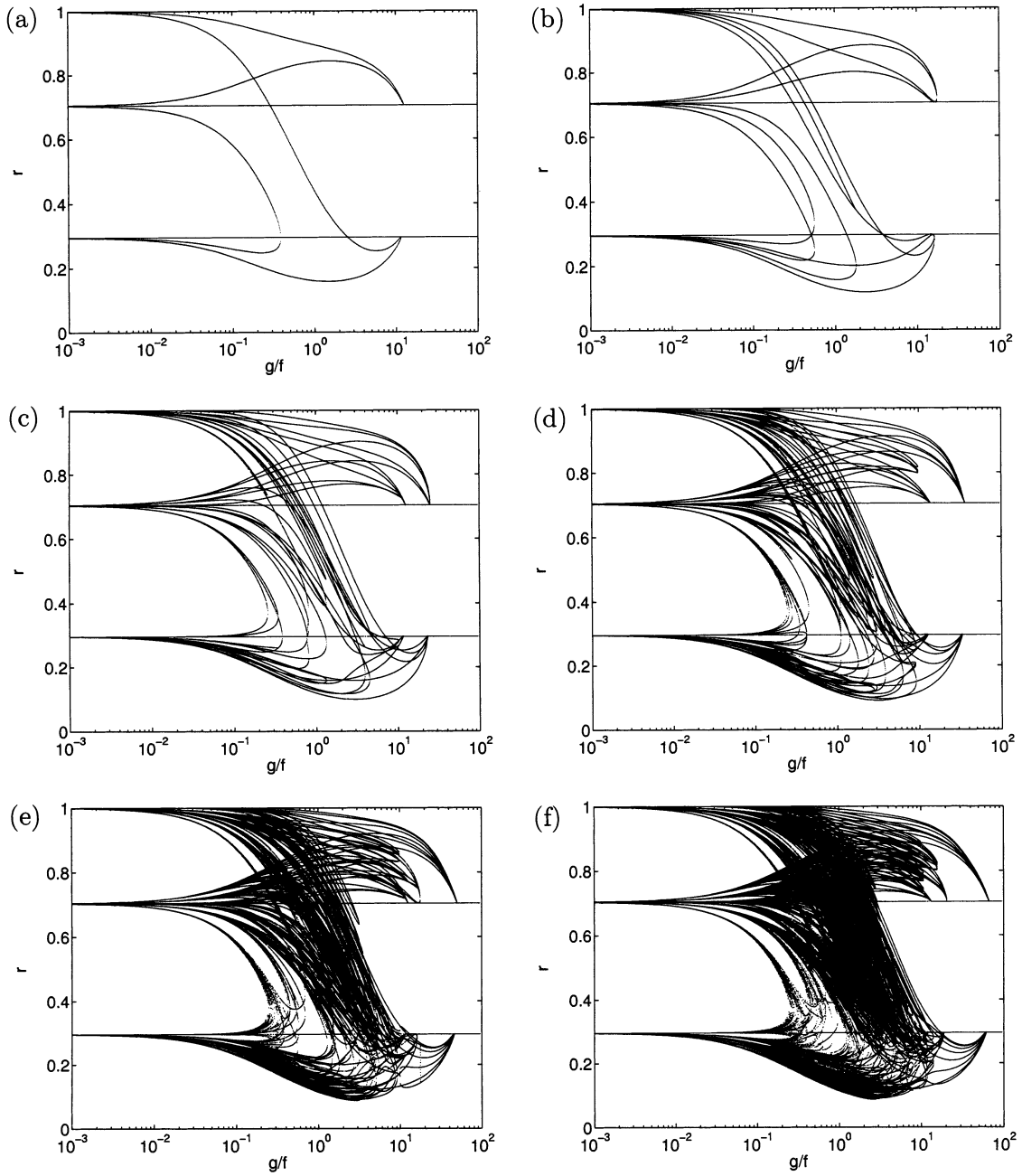

Figure 11. Bifurcation diagram of r vs g/f for bidirectional ring networks with $k = 25$, $d = 0.1$, and $f = 0.002$. The number of CSTRs in the network is (a) 2, (b) 3, (c) 4, (d) 5, (e) 6, and (f) 7. Unstable steady states are indicated with light lines. There are no stable steady states. The two horizontal lines represent the single-CSTR steady states.

states between $g/f \approx 9.98$ and $g/f \approx 19.88$, and the 10-CSTR network has stable steady states between $g/f \approx 7.54$ and $g/f \approx 28.16$. A near-continuum of steady states exists at certain interconnection flow rates. The 9-CSTR and 10-CSTR networks display the same gradient spatial patterns of resource and species concentrations and crossing of the lowest two stable steady states as those in the previous cases.

6. Dynamic Behavior of Bidirectional Networks

Next, the dynamic behavior of several network configurations is investigated through a series of computational experiments. For each numerical simulation, the feed flow rate to all reactors is manipulated to explore the boundaries of the stable regions of the bifurcation structure. The interconnection flow rate is kept constant in all cases, while the feed flow rate is ramped up or down from an initial to a final value.

6.1. Three-CSTR Network. In single- and double-CSTR systems,[35] the stable steady state may become unstable through a Hopf bifurcation, resulting in a stable limit cycle around the unstable branch. Perturbing the bifurcation parameter beyond the stable limit cycle region will result in the limit cycle becoming unstable and, ultimately, species washout. Similar behavior is observed in larger networks.

The three-CSTR network with bidirectional flow rates has a single pair of stable steady states at low feed flow rates, as can be seen in Figure 3b. For the value of $f \approx 0.004\,813$, the network resource concentrations are $(r_1, r_2, r_3) \approx (0.7182, 0.066\,59, 0.7182)$ and the species concentrations are $(p_1, p_2, p_3) \approx (0.001\,720, 0.065\,30, 0.001\,720)$. The network stable steady states in this

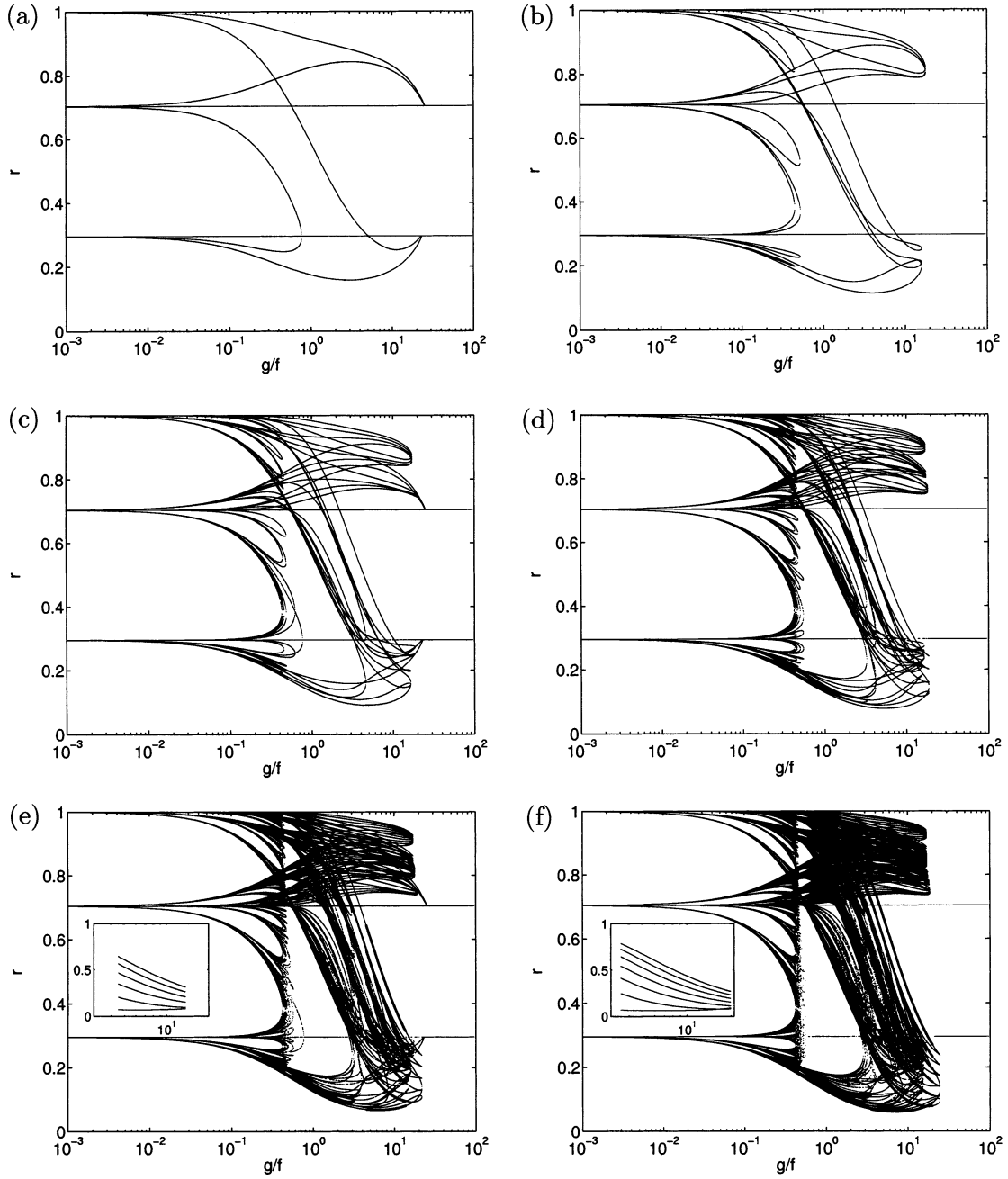

Figure 12. Bifurcation diagram of r vs g/f for unidirectional ring networks with $k = 25$, $d = 0.1$, and $f = 0.002$. The number of CSTRs in the network is (a) 2, (b) 3, (c) 4, (d) 5, (e) 6, and (f) 7. Unstable steady states are indicated with light lines, and stable steady states are indicated with dark lines. The insets of parts e and f are detailed views of the stable steady states only.

region always occur with two reactors in the high resource configuration and one reactor in the low resource configuration, although the precise ordering in the network is completely arbitrary.

If the feed flow rate is decreased from $f \approx 0.004\,813$ to $f \approx 0.004\,213$, the system is observed to pass through a Hopf bifurcation and onto a stable limit cycle (Figure 15a). For this example, the states of reactors 1 and 3 are synchronized, because of the starting conditions. Reducing the feed flow rate further will result in washout. Notice also that there is a gap between the regions of stability of the single-CSTR isola and the tip of the three-CSTR crescent (Figure 3b). Again starting from $f \approx 0.004\,813$, the feed flow rate is increased to $f \approx 0.006\,313$, which lies in this gap. The system collapses to the trivial steady state (Figure 15b). However, if the feed rate is increased slightly more to $f \approx 0.006\,538$, again starting from $f \approx 0.004\,813$, the system moves to a region of quasi-periodic oscillations (Figure 15c) with CSTR 1 and 3 synchronized on a very large period limit cycle and CSTR 2 oscillating quasi-periodically. When the feed rate is increased from $f \approx 0.004\,813$ to the periodic region of the single-CSTR case, $f \approx 0.006\,913$, all of the reactors will synchronize (Figure 15d). Finally, when the feed flow rate is increased further, the system moves to the stable steady state of the single-CSTR case (Figure 15e). Because of the symmetry of the network, the stable steady states of the three-CSTR network cannot be reached from the single-CSTR case simply by reducing the feed flow rate. Reduction of the feed flow rate beyond the periodic regime of the single-CSTR case will result in species washout. Thus, the process of moving from the three-CSTR stability region to that of the single CSTR is irreversible if the feed flow rate is

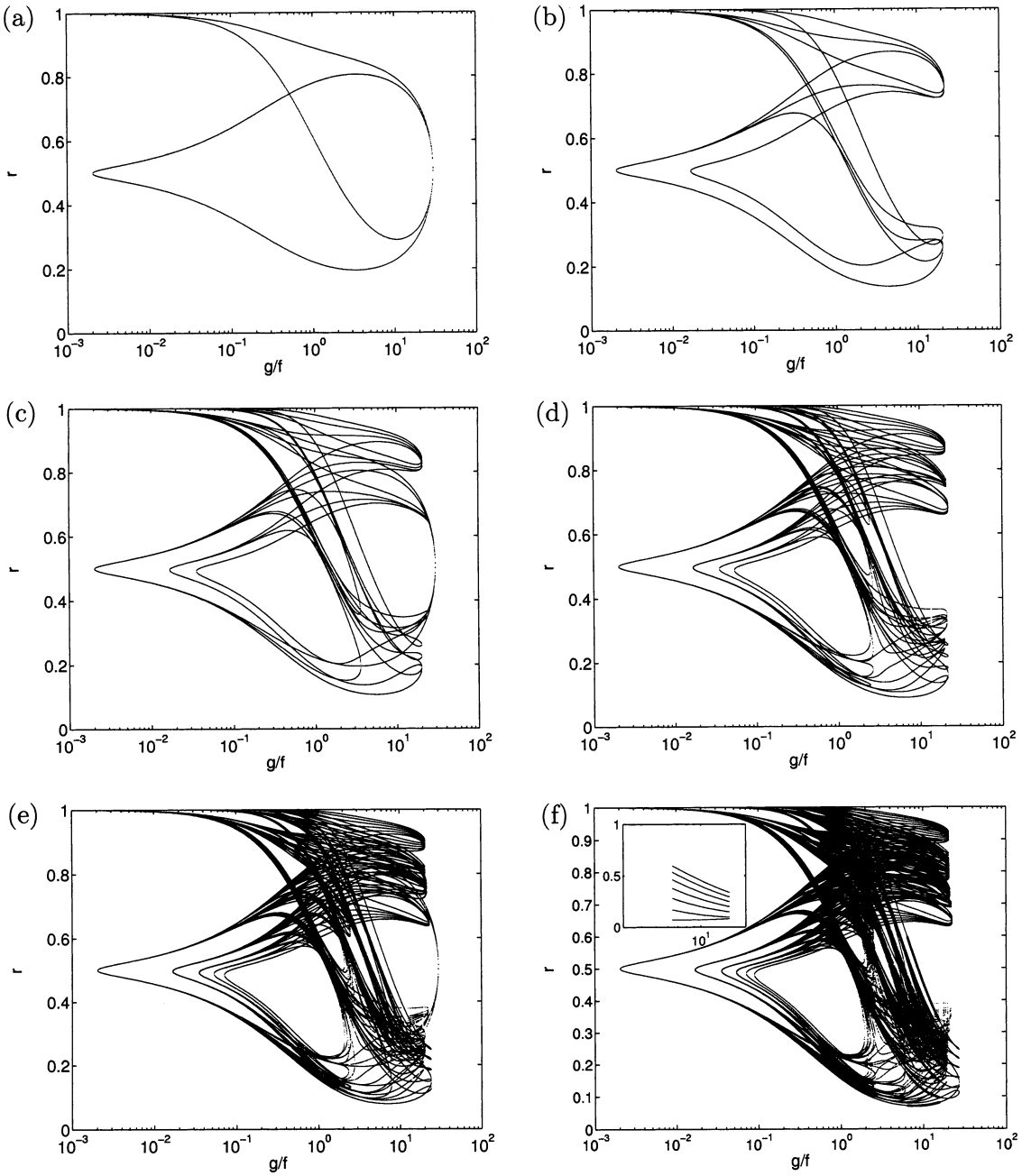

Figure 13. Bifurcation diagram of r vs g/f for unidirectional ring networks with $k = 25$, $d = 0.1$, and $f = 0.001\,65$. The number of CSTRs in the network is (a) 2, (b) 3, (c) 4, (d) 5, (e) 6, and (f) 7. Unstable steady states are indicated with light lines, and stable steady states are indicated with dark lines. The inset of part f is a detailed view of the stable steady states only.

the only manipulated variable. This property can be naturally generalized to higher order networks. For instance, if a six-CSTR network is locked to a three-CSTR regime via CSTR pairing, six-CSTR-specific states cannot be retrieved by uniformly changing the feed flow rate of the system. At high feed flow rates, though other stable regions are possible, the dynamics are governed by a simple ignition−extinction hysteresis and thus do not provide any significant dynamic information.

6.2. Four-CSTR Network. The four-CSTR bidirectional network has two combinations of stable steady states at low feed flow rates (Figure 3c). The first combination displays three distinct steady states. For the value of $f \approx 0.004\,625$, the network resource concentrations are $(r_1, r_2, r_3, r_4) \approx (0.7506, 0.8843, 0.7506, 0.066\,81)$ and the species concentrations are $(p_1, p_2, p_3, p_4) \approx (0.001\,692, 6.312 \times 10^{-5}, 0.001\,693, 0.069\,47)$. The spatial pattern consists of one high resource reactor surrounded by two identical lower resource reactors, followed by the lowest resource reactor. Steadily reducing the feed flow rate to $f \approx 0.004\,025$ results in the system moving to the periodic regime via a Hopf bifurcation (Figure 16a) similar to the three-CSTR network. Note that the dynamic concentration profiles for CSTRs 1 and 3 are identical, even though they do not directly exchange material via an interconnection flow rate.

If the feed flow rate is increased from $f \approx 0.004\,625$ to $f \approx 0.006\,425$, the network displays long period oscillations in CSTRs 1, 2, and 3 and a burstlike behavior in CSTR 4 (Figure 16b). Increasing the feed flow rate further from $f \approx 0.004\,625$ to $f \approx 0.007\,025$ causes the network to move to the single-CSTR periodic

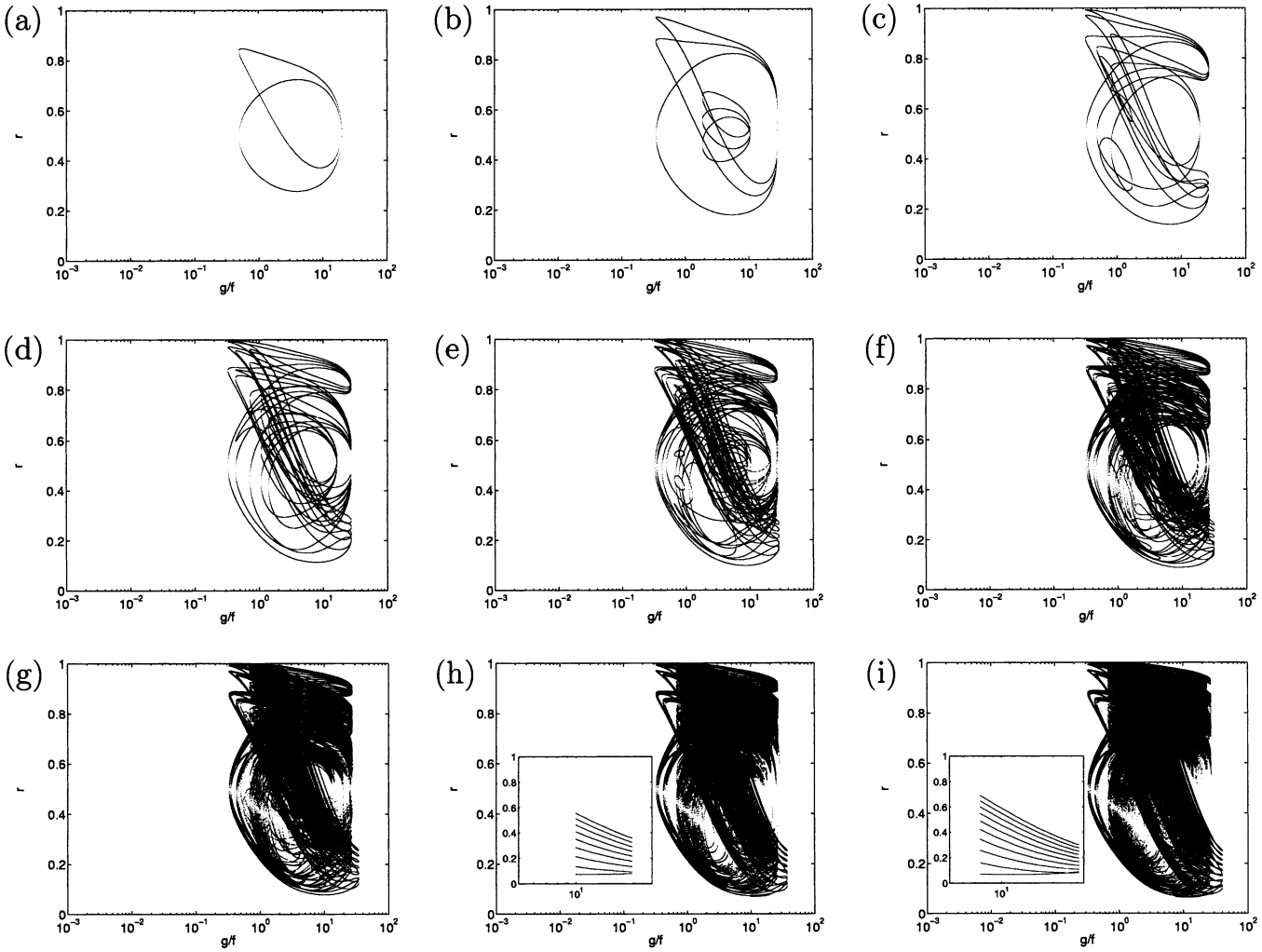

Figure 14. Bifurcation diagram of r vs g/f for unidirectional ring networks with $k = 25$, $d = 0.1$, and $f = 0.001\,25$. The number of CSTRs in the network is (a) 2, (b) 3, (c) 4, (d) 5, (e) 6, (f) 7, (g) 8, (h) 9, and (i) 10. Unstable steady states are indicated with light lines, and stable steady states are indicated with dark lines. The inset of parts h and i detailed views of the stable steady states only.

regime in which all reactors synchronize to a single-CSTR limit cycle (Figure 16c). A further increase in the feed flow rate results in the nontrivial single-CSTR stable steady state.

The second reactor configuration in the four-CSTR bidirectional network mimics a two-CSTR setup with twice the interconnection flow rate through locking neighboring CSTRs in pairs. For the value of $f \approx 0.006\,684$, the network resource concentrations are $(r_1, r_2, r_3, r_4) \approx (0.7743, 0.061\,29, 0.061\,29, 0.7743)$ and the species concentrations are $(p_1, p_2, p_3, p_4) \approx (0.002\,061, 0.0709, 0.0709, 0.002\,061)$. Note that, even though two stable steady states are possible in four reactors, the configuration is always a pair of pairs, as opposed to alternating high and low concentrations in the reactors. In this example, the first and fourth reactors are neighbors because of the toroidal network boundary conditions and are locked. The remaining reactors are also neighbors and are also locked.

Reducing the feed flow rate from $f \approx 0.006\,684$ to $f \approx 0.005\,334$ causes the system to pass through a Hopf bifurcation point and move into a periodic regime (Figure 16d). The limit cycles of reactors 1 and 4 and of reactors 2 and 3 are synchronized because the reactors were locked initially. If the feed flow rate is increased from $f \approx 0.006\,684$ to $f \approx 0.007\,344$, the system collapses to the nontrivial single-CSTR stable steady state (Figure 16e) because the stability region of the single-CSTR case begins just as the stability region of the four-CSTR network terminates. Note that, while for the previous spatial pattern of states in the four-CSTR network, the system could be moved to an oscillatory regime by increasing the flow rate, in this case, the ending and starting points of the stability region meet, and this does not allow for periodic behavior to occur.

7. Dynamic Behavior of Unidirectional Networks

7.1. Three-CSTR Network. When the interconnection flow rate is limited to one direction, the three-CSTR network develops a pair of nonoverlapping steady states at low feed flow rates consisting of one high species concentration, one intermediate species concentration, and one low species concentrations (Figure 8b). The inverse is true for the resource concentrations (Figure 7d). The ordering of the reactors proceeds from the highest species concentration to the lowest in the direction of the interconnection flow rate, that is, from CSTR 3 to CSTR 1. Again, note the rotational symmetry of the reactor indices. Here, the spatial concentration patterns depend on the initial condition.

For instance, at $f \approx 0.006\,011$, in a possible configuration, the network resource concentrations are $(r_1, r_2,$

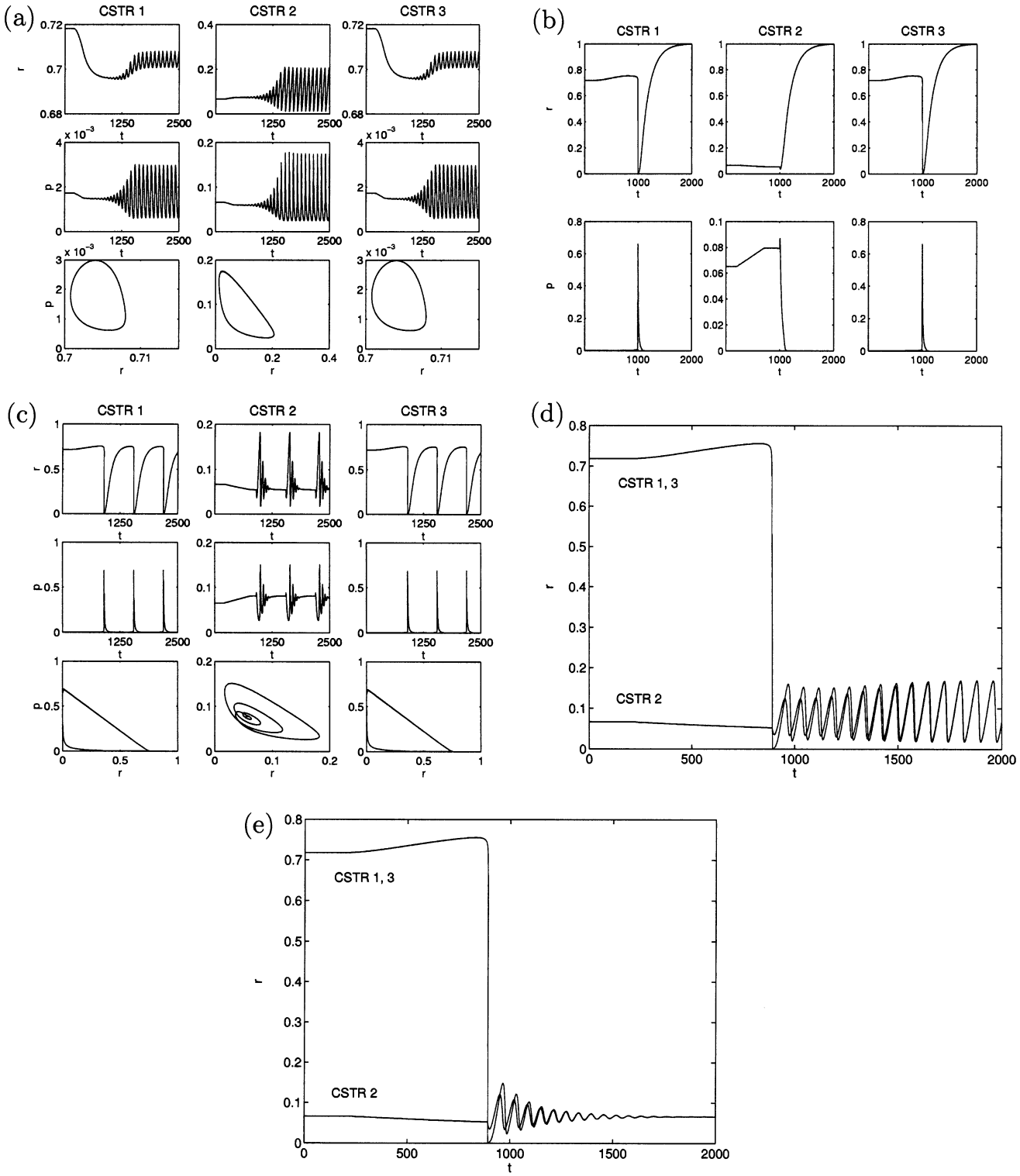

Figure 15. Dynamic behavior of bidirectional three-CSTR networks with $k = 25$, $d = 0.1$, and $g = 0.002$ as the feed flow rate is changed from f_1 to f_2: (a) $f_1 = 0.004\,813$, $f_2 = 0.004\,213$; (b) $f_1 = 0.004\,813$, $f_2 = 0.006\,313$; (c) $f_1 = 0.004\,813$, $f_2 = 0.006\,538$; (d) $f_1 = 0.004\,813$, $f_2 = 0.006\,913$; (e) $f_1 = 0.004\,813$, $f_2 = 0.007\,513$.

$r_3) \approx (0.063\,20, 0.9395, 0.7576)$ and the species concentrations are $(p_1, p_2, p_3) \approx (0.068\,36, 3.530 \times 10^{-5}, 0.001\,896)$. Thus, network stable steady states manifest a gradient pattern from highest to lowest species concentration in the direction of flow (CSTR 1 → CSTR 3 → CSTR 2).

If the feed flow rate is decreased from $f \approx 0.006\,011$ to $f \approx 0.004\,931$, the system is observed to pass through a Hopf bifurcation and onto a stable limit cycle (Figure 17a). If the feed flow rate is increased, starting from $f \approx 0.006\,011$ to $f \approx 0.006\,992$, the system moves to a region of quasi-periodic oscillations (Figure 17b). When the feed rate is increased to the periodic region of the single-CSTR case, all of the reactors synchronize. Figure 17c shows the behavior of the system starting from $f \approx 0.006\,011\,3$ and increasing to $f \approx 0.007\,061$. Finally, when the feed flow rate is increased further, the system moves to the nontrivial stable steady state of the single-

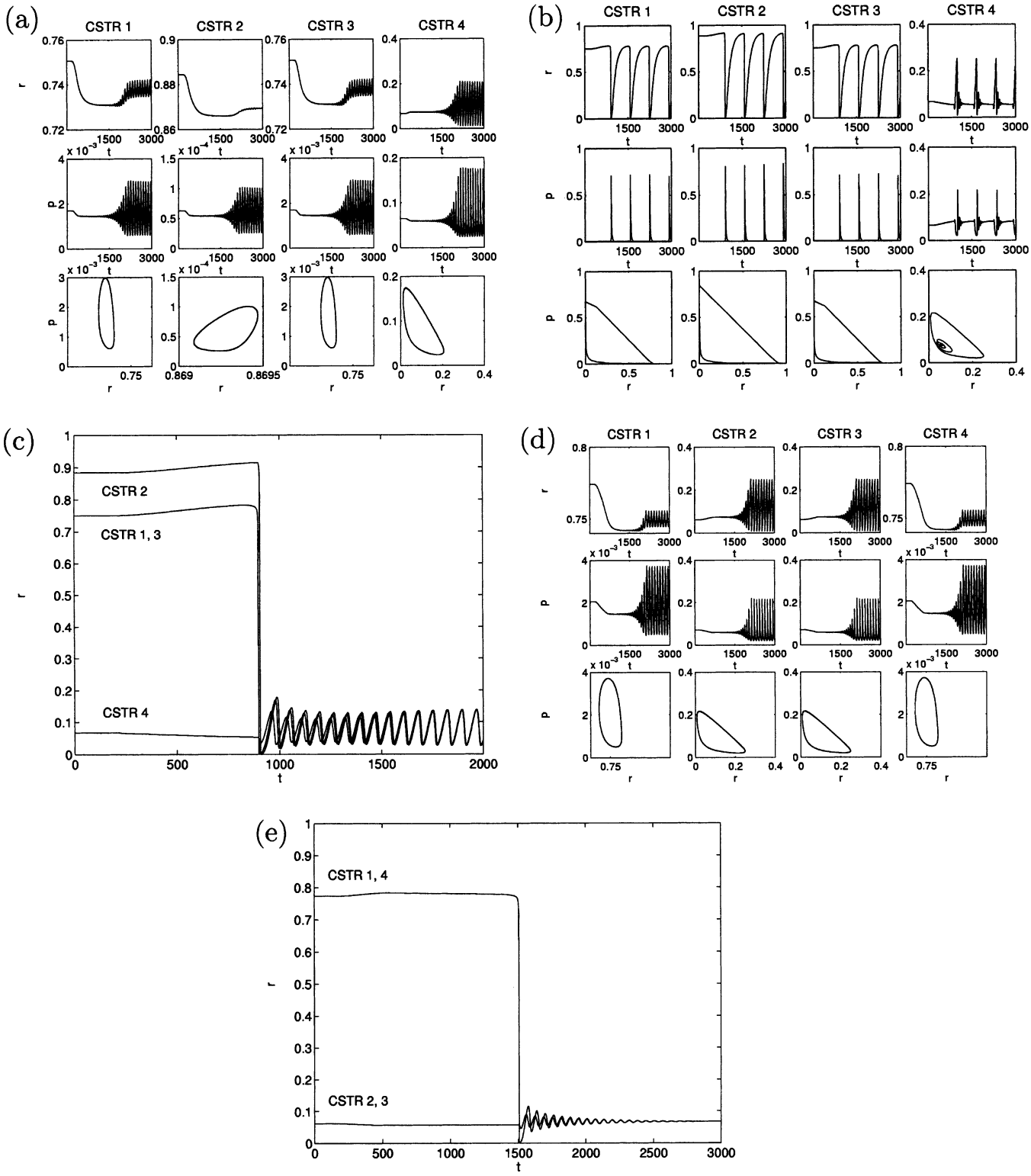

Figure 16. Dynamic behavior of bidirectional four-CSTR networks for $k = 25$, $d = 0.1$, and $g = 0.002$ as the feed flow rate is changed from f_1 to f_2: (a) $f_1 = 0.004\,625$, $f_2 = 0.004\,025$; (b) $f_1 = 0.004\,625$, $f_2 = 0.006\,425$; (c) $f_1 = 0.004\,625$, $f_2 = 0.007\,025$; (d) $f_1 = 0.006\,684$, $f_2 = 0.005\,334$; (e) $f_1 = 0.006\,684$, $f_2 = 0.007\,344$.

CSTR case. As in the bidirectional network, symmetry prevents the system from moving to the stable steady states of the three-CSTR unidirectional network from the single-CSTR case, simply by reducing the feed flow rate.

The three-CSTR unidirectional network has an additional stable steady-state configuration that begins at $f \approx 0.007\,121$ and overlaps the nontrivial single-CSTR steady state as f is increased. The stability region of the previous reactor configuration terminates just before $f \approx 0.007\,121$ and therefore does not overlap with the second reactor configuration. For the value of $f \approx 0.007\,301$, the network resource concentrations are $(r_1, r_2, r_3) \approx (0.057\,14, 0.7935, 0.067\,37)$ and the species concentrations are $(p_1, p_2, p_3) \approx (0.076\,49, 0.001\,666, 0.063\,52)$. Decreasing the feed flow rate on the second stable steady-state configuration moves the system to a quasi-periodic regime that is near the quasi-periodic

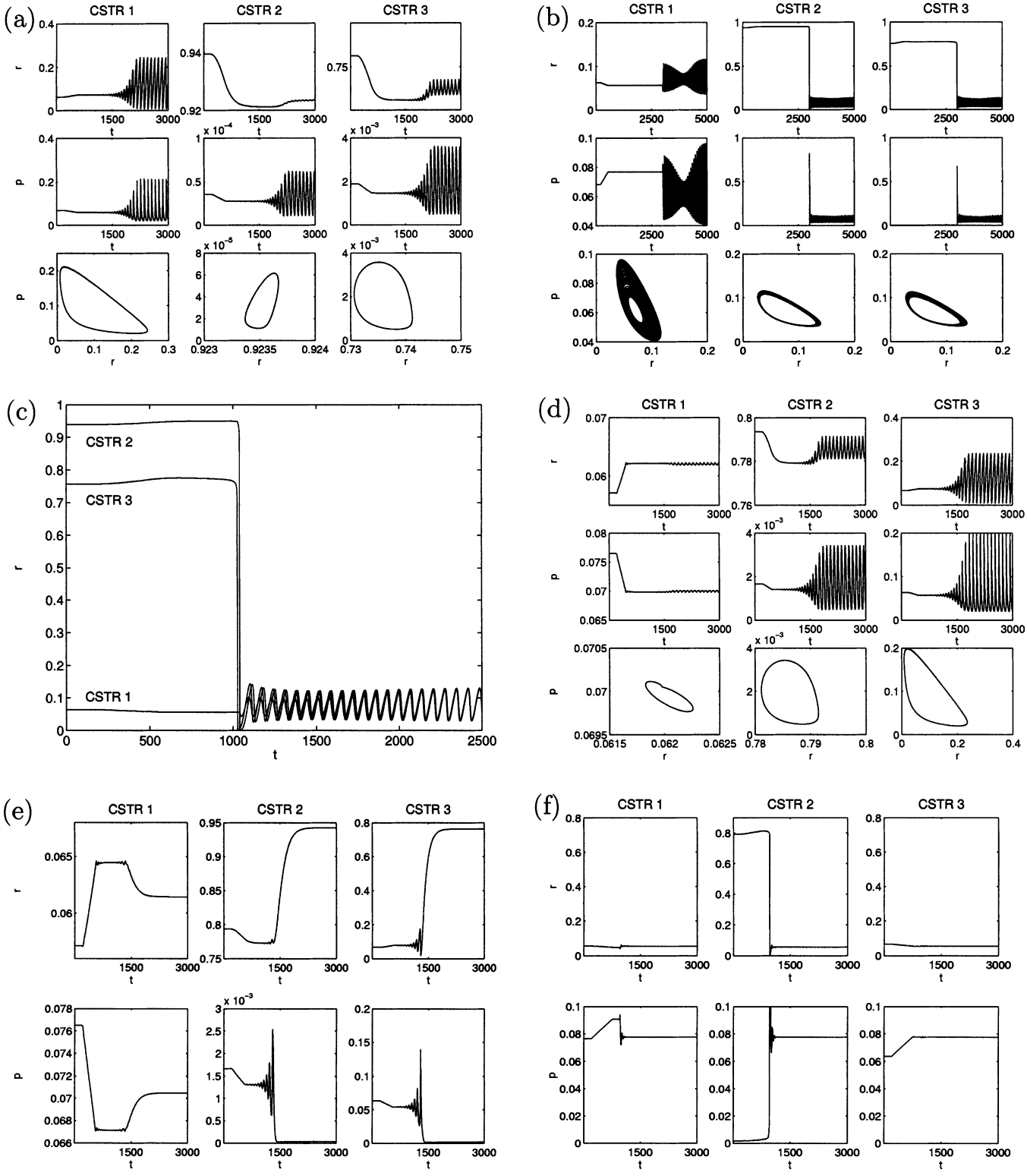

Figure 17. Dynamic behavior of unidirectional three-CSTR networks for $k = 25$, $d = 0.1$, and $g = 0.002$ as the feed flow rate is changed from f_1 to f_2: (a) $f_1 = 0.006\,011$, $f_2 = 0.004\,931$; (b) $f_1 = 0.006\,011$, $f_2 = 0.006\,992$; (c) $f_1 = 0.006\,011$, $f_2 = 0.007\,061$; (d) $f_1 = 0.007\,301$, $f_2 = 0.006\,251$; (e) $f_1 = 0.007\,301$, $f_2 = 0.006\,551$; (f) $f_1 = 0.007\,301$, $f_2 = 0.008\,951$.

regime of the first steady-state configuration. Figure 17d shows the system dynamics when the feed flow rate is decreased from $f \approx 0.007\,301$ to $f \approx 0.006\,551$. However, if the feed flow rate is further decreased from $f \approx 0.007\,301$ to $f \approx 0.006\,251$, the system moves to the first network stable steady-state configuration (Figure 17e). The network can move from the second stable steady-state configuration by decreasing the feed flow rate but not from the first to the second by increasing the feed flow rate because the first steady-state configuration will change to a quasi-periodic regime and then to the single-CSTR configuration if the feed flow rate is increased. If the feed flow rate is increased from $f \approx 0.007\,301$ to $f \approx 0.008\,951$, the system collapses to the nontrivial single-CSTR stable steady state (Figure 17f) because the stability region of the single-CSTR case overlaps the stability region of the three-CSTR networks.

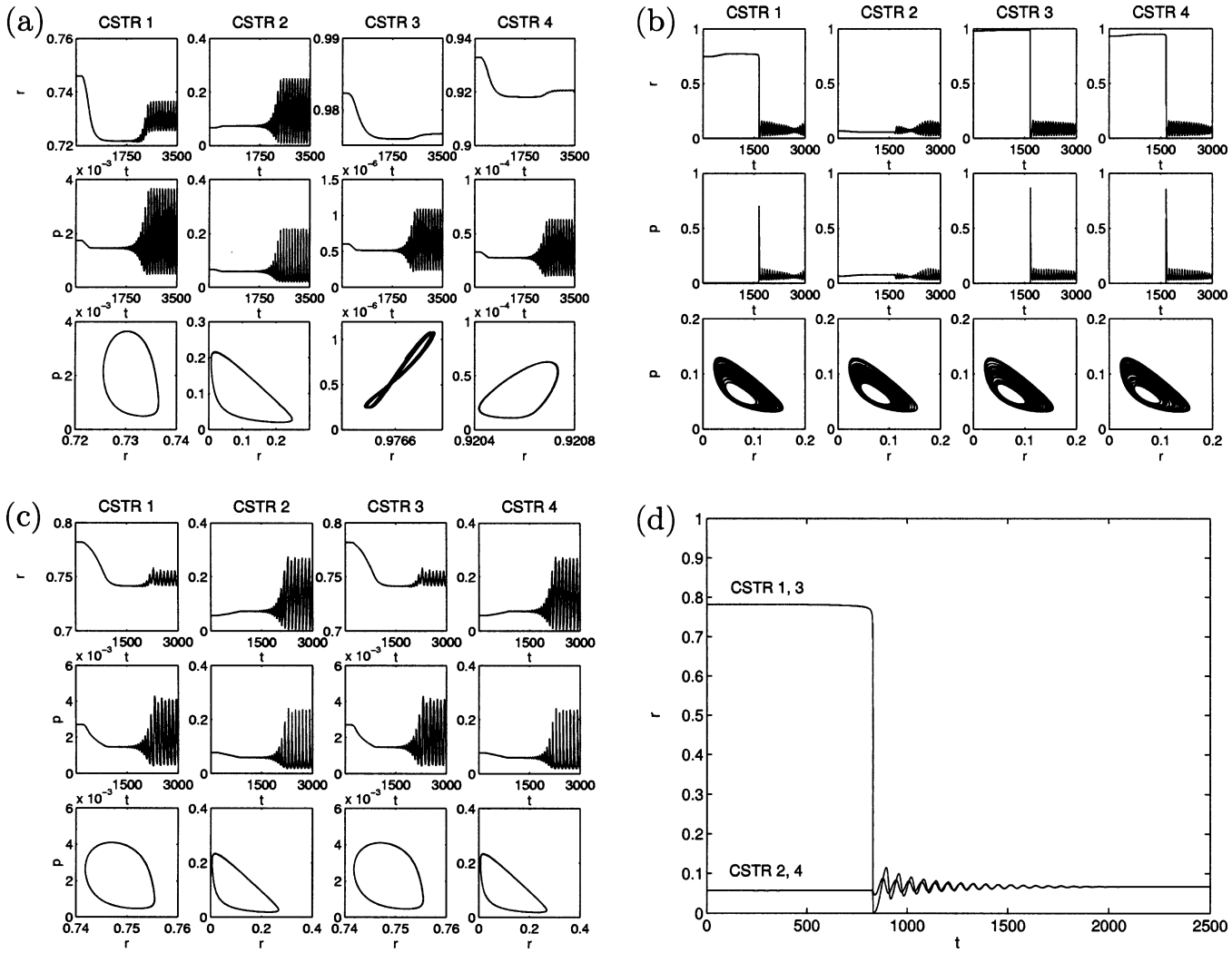

Figure 18. Dynamic behavior of unidirectional four-CSTR networks for $k = 25$, $d = 0.1$, and $g = 0.002$ as the feed flow rate is changed from f_1 to f_2: (a) $f_1 = 0.005\,577$, $f_2 = 0.004\,797$; (b) $f_1 = 0.005\,577$, $f_2 = 0.006\,927$; (c) $f_1 = 0.007\,301$, $f_2 = 0.005\,321$; (d) $f_1 = 0.007\,301$, $f_2 = 0.007\,361$.

7.2. Four-CSTR Network. Adding a fourth reactor to the three-CSTR unidirectional network allows the system to possess four different stable steady-state configurations at low feed flow rates (Figure 7c). With respect to the resource concentration, the network is stable in either a gradient configuration of high to low resource concentrations or alternating high and low resource concentrations. The unidirectional network differs from the bidirectional network in that the latter has a spatial gradient pattern that is independent of the flow direction and can emulate a two-CSTR network when two pairs of reactors synchronize. The pairing does not occur in the unidirectional case because interconnection flow rates limit communication between reactors to one direction.

For the value of $f \approx 0.005\,577$, the network resource concentrations are $(r_1, r_2, r_3, r_4) \approx (0.7459, 0.065\,72, 0.9823, 0.9329)$ and the species concentrations are $(p_1, p_2, p_3, p_4) \approx (0.001\,745, 0.065\,48, 6.077 \times 10^{-7}, 3.2658 \times 10^{-5})$. If the feed flow rate is decreased from $f \approx 0.005\,577$ to $f \approx 0.004\,797$, limit cycles appear in each reactor as the system moves from the stable regime across a Hopf bifurcation (Figure 18a). Decreasing the feed flow rate further results in species washout. Increasing the feed flow rate from $f \approx 0.005\,577$ to $f \approx 0.006\,927$ moves the system to a quasi-periodic regime (Figure 18b).

The second stable steady-state configuration for the four-CSTR unidirectional network consists of alternating high and low resource concentration reactors. For the value of $f \approx 0.007\,301$, the network resource concentrations are $(r_1, r_2, r_3, r_4) \approx (0.7820, 0.057\,28, 0.7820, 0.057\,28)$ and the species concentrations are $(p_1, p_2, p_3, p_4) \approx (0.002\,695, 0.076\,29, 0.002\,695, 0.076\,29)$. If the feed flow rate is decreased from $f \approx 0.007\,301$ to $f \approx 0.005\,321$, limit cycles appear in each reactor as the system moves from the stable regime across a Hopf bifurcation (Figure 18c). The limit cycles in CSTRs 1 and 3 are synchronized, as are the limit cycles in CSTRs 2 and 4, because of the starting conditions. The alternating reactors remain synchronous, despite the fact that they are not directly connected to each other. If the feed flow rate is increased from $f \approx 0.007\,301$ to $f \approx 0.007\,361$, the system collapses to the nontrivial single-CSTR stable steady state (Figure 18d) because the stability region of the single-CSTR case overlaps the stability region of the four-CSTR network.

The third stable steady-state configuration for the four-CSTR unidirectional network is a gradient spatial pattern. For the value of $f \approx 0.007\,637$, the network resource concentrations are $(r_1, r_2, r_3, r_4) \approx (0.7992, 0.064\,89, 0.6458, 0.5520)$ and the species concentrations are $(p_1, p_2, p_3, p_4) \approx (0.001\,802, 0.066\,34, 0.066\,43, 0.079\,27)$. If the feed flow rate is decreased from $f \approx$

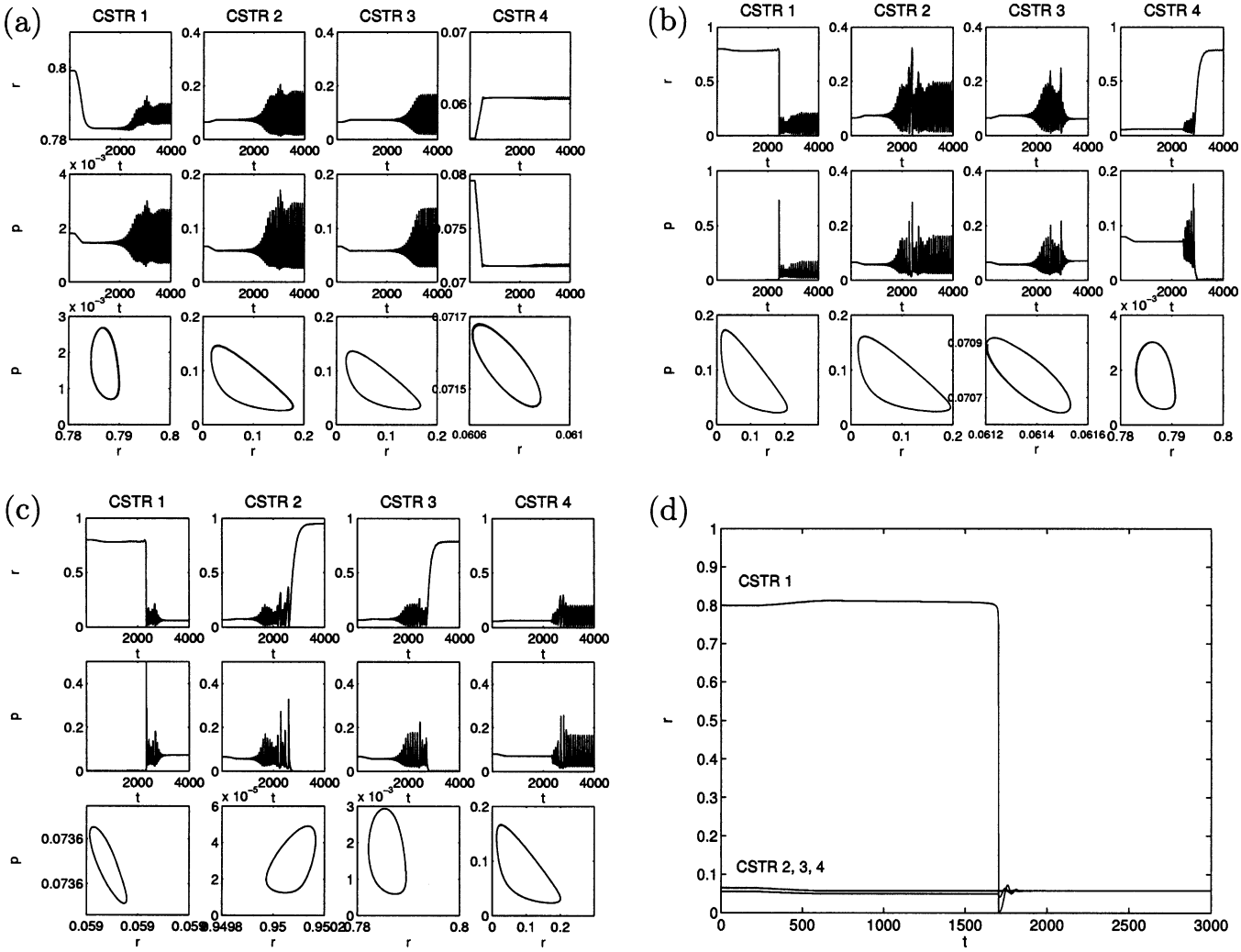

Figure 19. Dynamic behavior of unidirectional four-CSTR networks for $k = 25$, $d = 0.1$, and $g = 0.002$ as the feed flow rate is changed from f_1 to f_2: (a) $f_1 = 0.007\,637$, $f_2 = 0.006\,737$; (b) $f_1 = 0.007\,637$, $f_2 = 0.006\,647$; (c) $f_1 = 0.007\,637$, $f_2 = 0.006\,602$; (d) $f_1 = 0.007\,637$, $f_2 = 0.008\,747$.

0.007 637 to $f \approx 0.006\,737$, limit cycles appear in each reactor as the system moves from the stable regime across a Hopf bifurcation (Figure 19a). When the feed flow rate is decreased somewhat more from $f \approx 0.007\,637$ to $f \approx 0.006\,647$, the system again moves to a periodic regime but CSTRs 1 and 4 flip their states (Figure 19b). Reducing the feed flow rate even further from $f \approx 0.007\,637$ to $f \approx 0.006\,602$ results in the system moving to the periodic regime of the fourth stable steady-state configuration, which is again of the gradient variety (Figure 19c). If the feed flow rate is increased from $f \approx 0.007\,637$ to $f \approx 0.008\,747$, the system collapses to the nontrivial single-CSTR stable steady state (Figure 19d) because the stability region of the single-CSTR case again overlaps the stability region of the four-CSTR network.

8. Conclusions

The topography of interconnected CSTR networks is shown to drastically affect the steady-state bifurcation structure of the system. Spatial inhomogeneity of the network can be increased by increasing the number of reactors in the network as well as limiting the interconnection flow rates of the network to one direction. It has also been shown that the number of stable and unstable steady states increases with the inhomogeneity of the network.

Bidirectional networks contain spatial combinations of smaller networks when the number of reactors in the network is nonprime. A four-CSTR network can function as a two-CSTR network when two pairs of two reactors lock or as a single CSTR when all of them lock. The bifurcation structure of the four-CSTR network in the former case would be identical with that of a two-CSTR network, with the interconnection flows of the two-CSTR network twice those of the four-CSTR network. Additionally, the six-CSTR network can function both as a two-CSTR network when two sets of three reactors lock and as a three-CSTR network when three sets of two reactors lock, in addition to the omnipresent single-CSTR setup. Networks consisting of a prime number of reactors such as the three-, five-, and seven-CSTR networks do not have subsets other than the single-CSTR setup. This phenomenon is not observed in unidirectional networks because the broken symmetry of the interconnection flow rate prevents the reactors from synchronizing.

One interesting property of both bidirectional and unidirectional networks is that the network average resource concentrations have regions of stability with near-rational values for certain ranges of the feed flow

rate. For a network of I reactors, the average resource concentration may be i/I for $i = 1, ..., I$. The average network resource concentration is also observed to be nearly invariable with respect to the feed flow rate with the implication that the network may be operated over a large span of feed flow rates without causing the average concentration profiles to change. Note that the bifurcation diagrams are presented in the semilogarithmic scale; thus, the range of these nearly invariable concentrations spans more than an order of magnitude in the feed flow rate, f.

The existence of static spatial patterns in the network provides a capacity for the networks to function as computational devices. The direct analogy is to ANNs in which a specific set of system inputs results in an output determined by the interconnection of the network units. Thus, a network of reactors could be used to output a static concentration pattern based on the system inputs.

Spatial inhomogeneity affects the range of species concentrations that can be supported by the network. The six-CSTR bidirectional network can support species concentrations lower than 10^{-10}, and a unidirectional network of the same size can support species concentrations lower than 10^{-15}.

Numerical simulations show that CSTR networks possess a complex array of dynamic behavior. Reducing the feed flow rate causes the system to move from a stable steady state to a periodic regime via a Hopf bifurcation. Depending on the steady-state configuration, increasing the feed flow rate from the stable steady state may move the system to a quasi-periodic regime or the single-CSTR state. This transition can occur through multi-CSTR quasi-periodicity and the single-CSTR periodic regime, or the multi-CSTR stable steady state can collapse to the nontrivial single-CSTR stable steady state, if the stable branches overlap. Unidirectional networks have stable steady-state spatial configurations that can be reached from one another, whereas bidirectional networks do not. Additionally, both types of networks can also display chaotic behavior near the quasi-periodic regimes.

If only the feed flow rate is manipulated, the system cannot move to one of the multi-CSTR steady states if the network is situated on a single-CSTR steady state. Because of the symmetry in the single-CSTR case, the reactor states would have to be independently manipulated to achieve the multiple CSTR states. Such a transition would require simultaneous manipulation of both the feed flow rates and the interconnection flow rates.

Literature Cited

(1) Uppal, A.; Ray, W. On the Dynamic Behavior of Continuous Stirred Tank Reactors. *Chem. Eng. Sci.* **1974**, *30*, 967−985.

(2) Bilous, O.; Amundson, N. Chemical Reactor Stability and Sensitivity. *AIChE J.* **1955**, *1*, 513−521.

(3) Uppal, A.; Ray, W.; Poore, A. The Classification of the Dynamic Behavior of Continuous Stirred Tank Reactors−Influence of Reactor Residence Time. *Chem. Eng. Sci.* **1976**, *31*, 205−214.

(4) Farr, W.; Aris, R. Yet Who Would Have Thought the Old Man to Have Had So Much Blood in Him?−Reflections on the Multiplicity of Steady States of the Stirred Tank Reactor. *Chem. Eng. Sci.* **1986**, *41*, 1385−1402.

(5) Lin, K. Multiplicity, Stability and Dynamics for Isothermal Autocatalytic Reactions in CSTR. *Chem. Eng. Sci.* **1981**, *36*, 1447−1452.

(6) Gray, P.; Scott, S. Absence of Restrictions on Permissible Paths for Changing the Efficiencies of Operation of Flow Reactors. *J. Phys. Chem.* **1983**, *87*, 1835−1838.

(7) Gray, P.; Scott, S. Autocatalytic Reactions in the Isothermal, Continuous Stirred Tank Reactor: Oscillations and Instabilities in the System A + 2B → 3B; B → C. *Chem. Eng. Sci.* **1984**, *39*, 1087−1097.

(8) Gray, P.; Scott, S. Autocatalytic Reactions in the Isothermal, Continuous Stirred Tank Reactor: Isolas and Other Forms of Multistability. *Chem. Eng. Sci.* **1983**, *38*, 29−43.

(9) Scott S. Reversible Autocatalytic Reactions in an Isothermal CSTR: Multiplicity, Stability and Relaxation Times. *Chem. Eng. Sci.* **1983**, *38*, 1701−1708.

(10) Lynch, D. Chaotic Behavior of Reaction Systems: Parallel Cubic Autocatalators. *Chem. Eng. Sci.* **1992**, *47*, 347−355.

(11) Lynch, D. Chaotic Behavior of Reaction Systems: Mixed Cubic and Quadratic Autocatalators. *Chem. Eng. Sci.* **1992**, *47*, 4435−4444.

(12) Guderian, A.; Dechert, G.; Zeyer, K.; Schneider, F. Stochastic Resonance in Chemistry. 1. The Belousov−Zhabotinsky Reaction. *J. Phys. Chem.* **1996**, *100*, 4437−4441.

(13) Forster, M.; Merget, M.; Schneider, F. Stochastic Resonance in Chemistry 2. The Peroxidase−Oxidase Reaction. *J. Phys. Chem.* **1996**, *100*, 4442−4447.

(14) Hohmann, W.; Muller, J.; Schneider, F. Stochastic Resonance in Chemistry. 3. The Minimal-Bromate Reaction. *J. Phys. Chem.* **1996**, *100*, 5388−5392.

(15) Birol, I.; Teymour, F. Statics and dynamics of multiple cubic autocatalytic reactions. *Phys. D* **2000**, *144*, 279−297.

(16) Chaivorapoj, W.; Birol, I.; Teymour, F. Competition Between Robust and Nonrobust Autocatalytic Replicators. *Ind. Eng. Chem. Res.* **2002**, *41*, 3630−3641.

(17) Chaivorapoj, W.; Birol, I.; Cinar, A.; Teymour, F. Feedback Control of a Continuous-Flow Stirred Tank Reactor with Competing Autocatalators. *Ind. Eng. Chem. Res.* **2003**, *42*, 3765−3785.

(18) Teymour, F. Nonlinear Dynamics in Polymeric Systems. In *ACS Symposium Series*; Pojman, J., Tran-Cong-Miyata, Q., Eds.; American Chemical Society: Washington, DC, 2003; Vol. 869, Chapter 24.

(19) Lee, D.; Chang, P.; Mou, C. Micromixing Effects on Autocatalytic Reactions in a Stirred Tank: The Random Replacement IEM Model. *J. Phys. Chem. A* **1997**, *101*, 1854−1858.

(20) Nakajima, K.; Sawada, Y. Experimental studies on the weak coupling of oscillatory chemical reaction systems. *J. Chem. Phys.* **1980**, *72*, 2231−2234.

(21) Nevoral, V.; Votrubova, V.; Hassal, P.; Schreiberova, L.; Marek, M. Synchronization of Oscillations and Propagation of Excitations in Circular and Linear Arrays of Coupled CSTRs. *J. Phys. Chem. A* **1997**, *101*, 4954−4965.

(22) Votrubova, V.; Hasal, P.; Schreiberova, L.; Marek, M. Dynamical Patterns in Arrays of Coupled Oscillators and Exitators. *J. Phys. Chem. A* **1998**, *102*, 1318−1328.

(23) Yoshimoto, M.; Yoshikawa, K.; Mori, Y. Coupling among three chemical oscillators: Synchronization, phase death, and frustration. *Phys. Rev. E* **1993**, *47*, 864−874.

(24) Lekebusch, A.; Schneider, F. Two Biochemical Oscillators Coupled by Mass Exchange. *J. Phys. Chem. B* **1997**, *101*, 9838−9843.

(25) Yoshikawa, K.; Fukunaga, K. A tri-phasic mode is stable when three non-linear oscillators interact with each other. *Chem. Phys. Lett.* **1990**, *174*, 203−207.

(26) Hjelmfelt, A.; Ross, J. Mass-coupled Chemical Systems With Computational Properties. *J. Phys. Chem.* **1993**, *97*, 7988−7992.

(27) Kuramoto, Y. *Chemical Oscillations, Waves, and Turbulence*; Springer: New York, 1984.

(28) Laplante, J.; Pemberton, M.; Hjelmfelt, A.; Ross, J. Experiments on Pattern Recognition by Chemical Kinetics. *J. Phys. Chem.* **1995**, *99*, 10063−10065.

(29) Haykin, S. *Neural Networks: A Comprehensive Foundation*; Prentice Hall: Englewood Cliffs, NJ, 1999.

(30) Dechert, G.; Zeyer, K.; Lebender, D.; Schneider, F. Recognition of Phase Patterns in a Chemical Reactor Network. *J. Phys. Chem.* **1996**, *100*, 19043−19048.

(31) Hohmann, W.; Schinor, N.; Kraus, M.; Schneider, F. Electrically Coupled Chemical Oscillators and Their Action Potentials. *J. Phys. Chem. A* **1999**, *103*, 5742−5748.

(32) Sakurai, T.; Mihaliuk, E.; Chirila, F.; Showalter, K. Design and Control of Wave Propagation Patterns in Excitable Media. *Science* **2002**, *296*, 2009−2012.

(33) Strogatz, S. Exploring complex networks. *Nature* **2001**, *410*, 268−276.

(34) Taylor, M.; Kevrekidis, I. Couple, Double, Toil and Trouble: A Computer Assisted Study of Two Coupled CSTRs. *Chem. Eng. Sci.* **1993**, *48*, 2129−2149.

(35) Birol, I.; Parulekar, S.; Teymour, F. Effect of environment partitioning on the survival and coexistence of autocatalytic replicators. *Phys. Rev. E* **2002**, *66*, 051916.

(36) Doedel, E. AUTO: A Program for the Automatic Bifurcation Analysis of Autonomous Systems. *Congr. Num.* **1981**, *30*, 265−284.

(37) Kuznetsov, Y.; Levitin, V.; Skovoroda, A. *Continuation of stationary solutions to evolution problems in CONTENT*; Technical Report AMR9611; Centrum voor Wiskunde en Informatica: Amsterdam, The Netherlands, 1996.

(38) Ourique, C.; Biscaia, E.; Pinto, J. The use of particle swarm optimization for dynamical analysis in chemical processes. *Comput. Chem. Eng.* **2002**, *26*, 1783−1793.

(39) Hindmarsh, A.; Taylor, A. *PVODE and KINSOL: Parallel software for differential and nonlinear systems*; Technical Report UCRL-ID-129739; Lawrence Livermore National Laboratory: Livermore, CA, 1998.

Received for review November 4, 2003
Revised manuscript received April 16, 2004
Accepted April 22, 2004

IE030802D